Chapter 1

Introduction

Mathematically a dynamical system consists of two elements "dynamics" and "state". Dynamics are rules, describing how a system evolves. States are initial conditions telling us how a system starts, or they give information about the system in a certain situation [1]. Most successful rules that can model natural systems are differential equations, which many theories of physics employ. This is why the mathematician V.I. Arnold says that differential equations are the basis of scientific mathematical philosophy, which began with Sir Isaac Newton's mechanics and calculus and continues to the present day.

Studying physical nature by means of mathematical modelling attempts to understand and predict natural phenomenon. Traditionally, models are differential equations and solutions of them give rise to "*trajectories*" that explain the motion of a certain system like the position of a comet or when the next solar eclipse will take place given particular initial conditions. Geometrically speaking a differential equation is a *vector field* on a manifold, where a vector field is a rule that smoothly assigns a vector to each point on the manifold. Each point on the manifold represents an individual *state*, or a possible initial condition, of the system and the collection of those points form *phase-space*. The system is called *deterministic* if both future and past states are uniquely determined by its present state. From a classical point of view all physical systems are deterministic and this determinism implies full predictibility.

The study of *chaos* in classical mechanics originates in applied mathematics and mathematical physics. This dates back to the work of French mathematician, astronomer,

and physicist Henri Poincaré. In particular he studied the three-body problem of the Moon orbiting around the Earth under the perturbation of the Sun one hundred years ago [2]. Poincaré discovered chaotic behavior in the three body problem and showed that the deterministic approach explained above is wrong. No matter how intelligent we are, we will not be able to predict the complete evolution of chaotic systems. In a closed form (bounded) solution we could expect any small change in the initial conditions to produce a proportional change in the well predicted deterministic trajectories. But in a chaotic system, nearby trajectories can diverge in the long term. This implies that, a chaotic system contains two conflicting concepts determinism and unpredictibility. Equations that model a natural system are deterministic by formulation but they are unpredictible by means of "*sensitive dependence on initial conditions*". Another point of view is that even a perfect knowledge of a system is not sufficient to solve it exactly. The study of these statements belong to several fundamental branches of pure physics.

Strong non-linear systems may evolve in a chaotic fashion.Their analysis and prediction of their dynamics are not an easy task. With the help of modern dynamical system theory, perturbation theory, bifurcation theory, differential geometry, topology and digital computers, a huge scientific discipline, nonlinear dynamics was placed among other fields of pure and applied sciences even in engineering, biological and social sciences.

In this thesis our attention is on ideas rather than deep mathematical proofs. Our main topic is chaotic motion in Hamiltonian Dynamical Systems. The absence of invariant tori and constants of motion in phase space break the symmetry and make the systems non-integrable. In other words non-integrable systems exhibit chaotic properties. Even very simple systems, such as a double-pendulum shows chaotic behaviour.

Geodesic flow in inhomogeneous pp-waves, where geodesic equations are very *sensitive to the initial conditions,* is popularly known as dynamical *chaos* . Dynamics in inhomogeneous pp-wave space-times show chaotic behavior. Generated Hamiltonians from these space-times, seem to represent non-integrable systems.

1.1 Hamiltonian Systems

Conservative systems are loosely called Hamiltonian systems. The mechanics of Hamilton and Jacobi is an elegant way to treat mechanical systems, largely derived from 18th century celestial mechanics. The modern theory of Hamiltonian Systems has been developed under two important schools; on one hand there are the numerical calculations of Hènon-Heiles, Ollongren, Contopoulos, on the other hand there is the theorem of Kolmogorov, Arnold and Moser (KAM).

1.1.1 Phase Space and Its Hamiltonian

We expect Newton's Second Law to remain valid under circumstances undreamt of by Newton. The second chapter of Newton's Principia introduced his Second Law which is still a profound law of nature telling us :[2]

> "The rate of the momentum with time has the same direction and it is proportional to the applied force". (Notice that Newton does not state the Second Law in the form of force and acceleration which most textbooks do)

The idea of phase-space is already defined in Newton's Principia. Therefore the representation space for the development of the dynamical system, called *phase space*, at time t is specified by its momentum p_i and postion q_i , rather than its velocity $\dot{q_i}$ and its position q_i as is done in the Lagrangian formalism. We could start by defining the Lagrangian of the system and make a *Legendre transformation* to its Hamiltonian [3]

$$p_i = \frac{\partial L(q_i, \dot{q_i}, t)}{\partial \dot{q_i}}, \tag{1.1}$$

$$H(p, q, t) = \Sigma \dot{q_i} \frac{\partial L(q_i, \dot{q_i}, t)}{\partial \dot{q_i}} - L(q_i, \dot{q_i}, t) \tag{1.2}$$

The space composed of points specified by the n momenta p_i and n coordinates q_i is called the phase-space. In abstract mathematical terminology this is the cotangent bundle for the manifold in which dynamical system moves. [4] Hamilton's canonical

equations of motion become [3]

$$\frac{dp_i}{dt} = -\frac{\partial H(p,q,t)}{\partial q_i} \tag{1.3}$$

$$\frac{dq_i}{dt} = \frac{\partial H(p,q,t)}{\partial p_i} \tag{1.4}$$

$$\frac{dH(p,q,t)}{dt} = \frac{\partial H(p,q,t)}{\partial q_i}\frac{dq_i}{dt} + \frac{\partial H(p,q,t)}{\partial p_i}\frac{dp_i}{dt} \equiv 0 \Longrightarrow H(p,q,t) = const. \tag{1.5}$$

There are two sets of first- order equations, rather than one set of second-order equations in the Newtonian tradition. The solutions of, these sets are *vector-fields* in phase space, and define a *flow* in phase-space. Conservation of energy in Hamiltonian mechanics requires that the value of $H(p,q,t)$ remain constant along any trajectory and implies

$$\frac{\partial H(p,q,t)}{\partial t} = 0, H(p,q,t) = E \tag{1.6}$$

Conservative Hamiltonians gives rise to the following statement of Liouville's Theorem [3];

> " The flow generated by a time-independent Hamiltonian system (an autonomous system) is volume preserving in phase-space"

This theorem is fundamental in statistical mechanics, as the density of a dynamical system D in the neighborhood of the system in phase-space remains constant. Mathematically speaking

$$\frac{dD}{dt} = \{D, H(p,q,t)\} + \frac{\partial D}{\partial t} \tag{1.7}$$

(Brackets { } are called Poisson bracket ; they play a crucial role in the dynamics of particles in phase-space,). we shall see that Liouville's theorem restricts geodesic motion to certain regions, or channels.

1.2 Integrable Systems

Traditional symmetric or regular systems lead to integribility. Since our discussion is mainly about chaotic dynamical systems, questions like "How or when systems would behave in a chaotic sense?" are unavoidable. Before proceeding we should define some concepts without proofs but with more care on ideas.

1.2.1 Constants of Motion and Poisson Brackets

We found that integrable systems are distinguished by having other *constants of motion* in addition to energy. Finding them is not an easy task and in many cases it is very difficult or impossible. Constants of motion generate *invariant tori* in phase space. Suppose we can write the Hamiltonian of a system and its equation of motions in the above framework. Then a function F(p_i,q_i) is defined as follows [4]

$$0 = \frac{d}{dt}F(p_i, q_i) = \frac{\partial F}{\partial p_i}\frac{dp_i}{dt} + \frac{\partial F}{\partial q_i}\frac{dq_i}{dt} \tag{1.8}$$

$$0 = \frac{\partial H}{\partial p_i}\frac{\partial F}{\partial q_i} - \frac{\partial H}{\partial q_i}\frac{\partial F}{\partial p_i} = \{H, F\} \tag{1.9}$$

Poisson bracket { H , F } can be computed for any two functions in phase-space and vanishing of Poisson bracket between Hamiltonian H and the function F makes F a constant of motion. In this sense the Hamiltonian itself is a constant of motion because {H,H} vanishes to zero.

Vanishing of Poisson bracket is have a geometric interpretation: the vector field (-$\frac{\partial H}{\partial q}, \frac{\partial H}{\partial p}$) in phase space is tangent to the surface F(q,p) = constant. Conversely, the vector field (-$\frac{\partial F}{\partial q}, \frac{\partial F}{\partial p}$) is tangent to the energy surface H(p,q)=E. The trajectories flow in phase space on the intersection of these two surfaces.

There may be more than one constant of motion for a certain system and each constant of motion, F_i(q,p) = constant, satisfies a vanishing condition of its Poisson bracket with Hamiltonian. There constants should be independent.

A dynamical system with n degrees of freedom has a phase space of 2n dimensions.

If we could find k independent constants of motion including the energy surface Hamiltonian, then the trajectories are restricted to a (2n-k) dimensional sub-space of all phase space. If the Poisson bracket of two constants of motion vanish then these constants of motion are said to be "in involution". (or commute) [5]

$$\{F_x, F_y\} = \frac{\partial F_x}{\partial p_i}\frac{\partial F_y}{\partial q_i} - \frac{\partial F_x}{\partial q_i}\frac{\partial F_y}{\partial p_i} = 0$$

1.2.2 Invariant Tori and Action-Angle Variables

The most desired stiuation is reached when there are n constants of motion in involution, this condition implies that the trajectories are confined to an n-dimensional manifold, and by the theorem of topology *this manifold has the shape of an n-dimensional torus.* Each single trajectory flows inside such an *invariant torus.* The dynamical system is then called *integrable.* Also, finding n constants in involution implies integribility of the system or equivalently the possibility of finding explicit solutions of the equations of motions.

If the above conditions are satisfied, a special system of coordinates can be constructed in phase space, the action-angle variables. As shown in most text books of classical mechanics the transformation of an integrable system from the original coordinates (p,q) to the action angle variables (I,Θ), can be done by using Jacobi's theory of first-order partial differential equations [3,4,6]. Here I plays the role of momenta with respect to position angle Θ.

Canonical (symplectic) changes of coordinate are defined by,

$$\begin{aligned} I &= I(q_2, p_2), q_2 = Q_2(\Theta, I) \qquad (1.10) \\ \Theta &= \Theta(q_2, p_2), p_2 = P_2(\Theta, I) \\ H(q_1, p_1, q_2, p_2) &= H(q_1, p_{2,} Q_2(\Theta, I), P_2(\Theta, I)) = H(q, p, \Theta, I) = const. \qquad (1.11) \end{aligned}$$

We have dropped q_1, p_1 and Q_2, P_2 turn out to be 2π periodic in the reduced Hamilton's canonical equations

$$\frac{dp}{dt} = -\frac{\partial H(q, p, \Theta, I)}{\partial q}, \frac{d\Theta}{dt} = \frac{\partial H(q, p, \Theta, I)}{\partial I} \qquad (1.12)$$

$$\frac{dq}{dt} = \frac{\partial H(q,p,\Theta,I)}{\partial p}, \frac{dI}{dt} = -\frac{\partial H(q,p,\Theta,I)}{\partial \Theta} \tag{1.13}$$

Our corresponding action integral for closed loop C_i

$$I_i = \frac{1}{2\pi} \oint_{C_i} p dq$$

As soon as the invariant tori in phase space are recognized we can construct action-angle variables, and vice versa. Most of the recent work on chaos in classical mechanics, and in celestial mechanics starts with the search for integrability (invariant tori), or in astronomy for with finding action-angle variables.

1.3 The Origins of Chaos:Hamiltonian Systems

The Poincarè-Bendixon theorem says that there are no more than four kinds of behaviour for differential equations in planar vector fields, these possibilities are a *source*, *sink*, *saddle* and *limit cycle*. This implies no chaotic motion is possible in time independent planar vector fields. To obtain chaotic motion in a system of differential equations one needs three dimensions, that is, a vector field on a three dimensional manifold.[6]

The asymptotic motions ($t \longrightarrow \infty$)of a flow generates four types of behaviour, in order of increasing complexity these are *equilibrium points*, *periodic solutions*, *quasiperiodic solutions*, and *chaos*. The *equilibrium points* of a flow are constant, time independent solutions. The equilibrium solutions are located where the vector fields vanish. A *periodic solution* of a flow is a time dependent trajectory that returns to itself in time T, called the period. A *quasiperiodic solution* is a solution formed from the sum of periodic solutions with incommensurate periods (irrational ratio of two periods). If we could not correlate our asymtotic motion with the classes above, then the motion is by Poincare‘s definition chaotic.

Application of chaos theory and its tool box has huge ramifications in the manner of mathematical background. That is why we restrict the origin of chaos to Hamiltonian system's . After Poincare‘s foundations for chaos, Physics was changed by huge revolutions, firstly by General Relativity and than by Quantum Mechanics. After the discovery

of modern computers, the study of chaos has expanded. A study of third integrals by Hènon and Heiles in 1963 has been very influential because of the questions they raised. They studied Poincarè sections or Poincarè mappings of certain Hamiltonians. (The Hènon Heiles family will be discussed in section 3.2), their study is one of the origins of chaos theory. [5]

1.3.1 Surface of Section of Hènon-Heiles Type Hamiltonian

Poincarè found it difficult to visualize the three dimensional content of a bowl of noodles. Therefore, he proposed to make a two dimensional cut in such a way that no noodle is tangent to this "surface of section" Σ. To describe surface of section we can choose internal coordinates (p_2,q_2) that form a conjugate pair of momentum and position. Starting from any pair ($p_{2,0}$,$q_{2,0}$) serves as the initial condition for a trajectory at t=0 in Σ. This trajectory will intersect Σ again at a point ($p_{2,1}$,$q_{2,1}$) at time t_1, always at the fixed energy E. This process could be done on a computer with numerical integration of the equations of motions. [2]

Let us consider the following Hamiltonian dealt with by Hènon-Heiles [5], which we demostrate a surface-section for this type of Hamiltonian with different energies by numerical integration at $q_1 = 0$.

$$H(p_1, q_1, p_2, q_2) = \frac{1}{2}(p_1^2 + q_1^2) + \frac{1}{2}(p_2^2 + q_2^2) + q_1^2 q_2 - \frac{1}{3}q_2^3 \tag{1.14}$$

The system has two degrees of freedom and the Hamilton's equations lead to the system

$$\ddot{q_1} + q_1 = -2q_1q_2 \tag{1.15}$$

$$\ddot{q_2} + q_2 = -q_1^2 + q_2 \tag{1.16}$$

$$dot = \frac{d}{dt}, q_1(t) = q_1, q_2(t) = q_2$$

The system derived from the Hènon-Heiles Hamiltonian is integrated numerically to construct Poincarè-sections of the plane { p_2, q_2 } at $q_1 = 0$ with various constant energies.(E = 1/24,1/18,1/12,1/8,1/7,1/6) in figure 1.1. As We have provided a computational souce

code for how to generate such pictures in Appendix 1.1. The idea behind these sections is they help us to classify dynamics of the system for a certain constant energy. For example, on choosing E = 1/12, the transversal plane shows a regular pattern with 7 fixed points and closed curves around 4 of them. The fixes points correspond with periodic solutions, the closed curves correspond with tori.

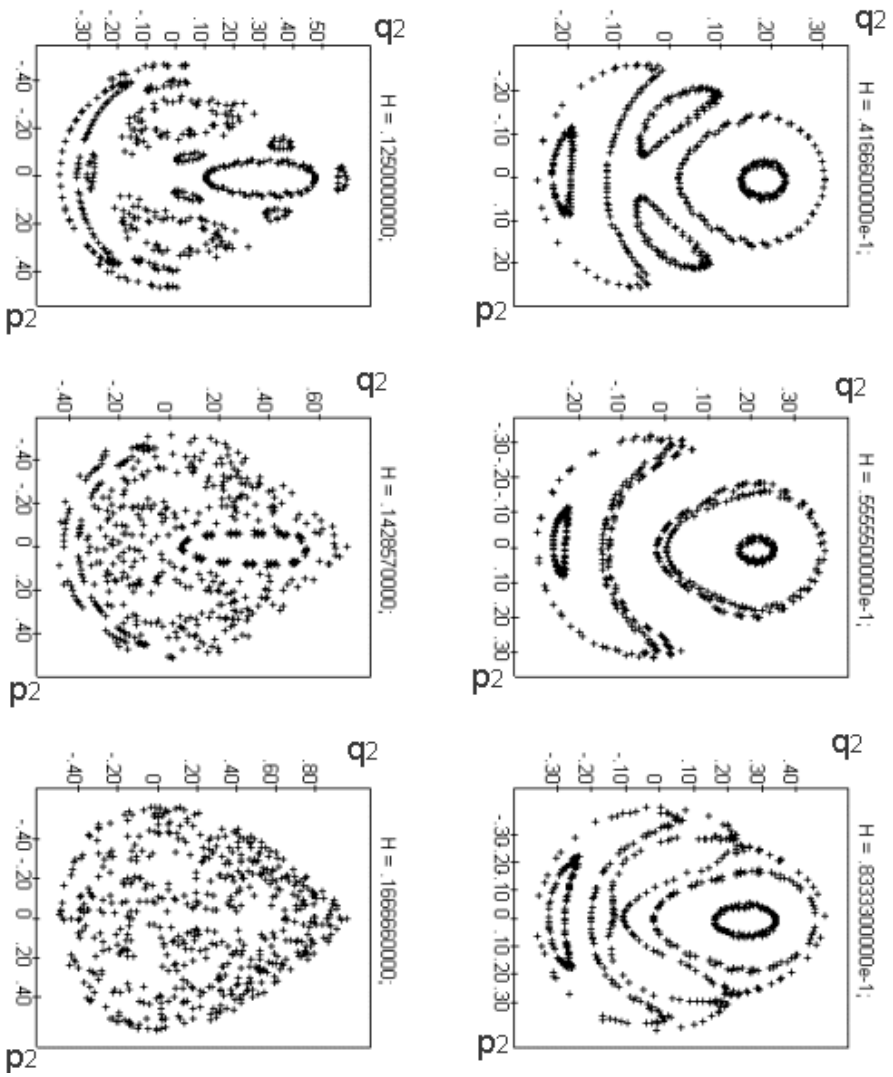

Figure 1-1: Poincarè sections of system that investigated by Hènon and Heiles in 1963 with various different constant energy surfaces.

Chapter 2

Geodesics in pp-waves

Studies of nonlinear phenomena and chaotic behaviour in general relativity have been done for different aspects using different approaches. Some examples include solutions to Einstein's equations (Found in a PhD thesis of Svend Rugh, 1990 from the Niels Bohr Institue appears as "Chaos in Einstein's Equations"), some cosmological models and complicated nonlinear models that occur in systems with coupled gravitational and scalar fields. Other types of investigations are for chaotic geodesic motions in given space-times like perturbed Schwarzshild and static axisymmetric geometry.[7] This thesis examines extensively a well known class of vacuum plane-fronted exact gravitational waves with parallel rays (pp-waves) which were found by Brinkmann in 1923 and gives an analysis of how chaos arrises. [7,8,9]

2.1 Plane-Fronted Gravitational Waves

Gravitational fields can propagate through empty space-time with the following field configurations [10] , they;

- move with speed of light along a straight line
- have a flat planar wave front
- are of finite durations.(for sandwich waves)

Planar wave solutions can be constructed with direction of motion along the x- axis and transverse direction defined by the (y-z)-plane with the following metric

$$-g_{\mu\nu}(\overrightarrow{x},t) = \begin{pmatrix} -1 & 0 & 0 & 0 \\ 0 & 1 & 0 & 0 \\ 0 & 0 & f^2(x,t) & 0 \\ 0 & 0 & 0 & g^2(x,t) \end{pmatrix} \tag{2.1}$$

The corresponding space-time line element is given by,

$$-ds^2 = -c^2dt^2 + dx^2 + f^2(x,t)dy^2 + g^2(x,t)dz^2 \tag{2.2}$$

These metrics

- are flat (Minkowskian) in the (x,t)-plane space-time
- are generally not flat in the y- and z- directions a space-time, and the value of the metric depends only on x.

The metric of vacuum pp-wave space-times can be written in a standard form [9]

$$ds^2 = 2d\zeta d\overline{\zeta} - 2dudv - (f+\overline{f})du^2 \tag{2.3}$$

where f (u,ζ) is an arbitrary function of the retard time u and complex coordinate ζ spanning the plane wave surface u = constant, when f is linear the metric (2.3) represents Minkowski universes, the simplest case for which (2.3) describes gravitational waves arises for f= h(u)ζ^2 where the arbitrary function h(u) characterizes the 'profile' of the wave. Solutions of these types are called homogenoeus pp-wave solutions. This simple example of an exact radiative space-time has also been used for the construction of sandwich and impulsive waves. We will investigate a more general case, geodesics in non-homogeneous vacuum pp-waves and demostrate their chaotic motion. Before driving geodesic equations from the metric (2.3) we need to know the corresponding Lagrangian of the system.

2.2 The Action Principle for a Relativistic Particle

Consider the world line of an ordinary particle (one that may or may not be free) having time-like curve [11]

$$ds^2 = c^2 d\tau^2 \tag{2.4}$$

Here, because proper time τ is an affine parameter, its square can be considered as a line-element, using symbolic notation with natural units c = 1.

$$d\tau^2 = g_{\alpha\beta} dx^\alpha dx^\beta \tag{2.5}$$

Using proper time τ as a parameter we can determine a unit vector pointing in the direction of time which is nothing but the four velocity U^α (tangent vector) satisfying normalizing condition

$$U^\alpha U_\alpha = \epsilon \tag{2.6}$$

$\epsilon = 1, 0, -1$ for time-like, null and spacelike geodesics respectively. The corresponding action

$$S = \int_{\tau_1}^{\tau_2} d\tau = \int_{\lambda_1}^{\lambda_2} \sqrt{g_{\alpha\beta} \frac{dx^\alpha}{d\lambda} \frac{dx^\beta}{d\lambda}} d\lambda \tag{2.7}$$

Since our affine parameter λ is the same as τ, this action turns out to be

$$S = \int_{\lambda_1}^{\lambda_2} L(x^\alpha, \frac{dx^\alpha}{d\lambda}) d\lambda \tag{2.8}$$

$$S = \int_{\tau_1}^{\tau_2} \sqrt{\{2 \frac{d\zeta}{d\tau} \frac{d\overline{\zeta}}{d\tau} - 2 \frac{du}{d\tau} \frac{dv}{d\tau} - (f + \overline{f})(\frac{du}{d\tau})^2\}} d\tau \tag{2.9}$$

Than the Lagrangian of the system for a metric time-like $\epsilon = 1$ metric can be written

$$L(\zeta, \overline{\zeta}, u, v) = \frac{d\zeta}{d\tau} \frac{d\overline{\zeta}}{d\tau} - \frac{du}{d\tau} \frac{dv}{d\tau} - \frac{1}{2}(f + \overline{f})(\frac{du}{d\tau})^2 = \frac{\epsilon}{2} \tag{2.10}$$

2.3 Derivation of Geodesic Equations

Equations that show how particle motion evolve with time (flow) can now be derived using Lagrangian (2.10) and the Euler-Lagrange equations [4] where dot denotes $\frac{d}{d\tau}$ and f(u,ζ)=f, Re-write the Lagrangian

$$L(\zeta,\overline{\zeta},u,v) = \dot{\zeta}\dot{\overline{\zeta}} - \dot{u}\dot{v} - \frac{1}{2}(f+\overline{f})(\dot{u})^2$$

The corresponding Euler-Lagrange equations are

$$\frac{d}{d\tau}\frac{\partial L}{\partial \dot{\zeta}} = \frac{\partial L}{\partial \zeta} \tag{2.11}$$

$$\frac{d}{d\tau}\frac{\partial L}{\partial \dot{\overline{\zeta}}} = \frac{\partial L}{\partial \overline{\zeta}} \tag{2.12}$$

$$\frac{d}{d\tau}\frac{\partial L}{\partial \dot{u}} = \frac{\partial L}{\partial u} \tag{2.13}$$

$$\frac{d}{d\tau}\frac{\partial L}{\partial \dot{v}} = \frac{\partial L}{\partial v} \tag{2.14}$$

Using (2.11)

$$\ddot{\zeta} = -\frac{1}{2}\overline{f}_{,\overline{\zeta}}\,(\dot{u})^2 \tag{2.15}$$

Using (2.12)

$$\ddot{\overline{\zeta}} = -\frac{1}{2}f_{,\zeta}\,(\dot{u})^2 \tag{2.16}$$

Using (2.14)

$$-\ddot{u} = 0 \rightarrow \dot{u} = const. = U \tag{2.17}$$

Using (2.13), and (2.17)

$$\ddot{v} = -\frac{1}{2}(f+\overline{f})_{,u}(\dot{u})^2 - (f_{,\zeta}\dot{\zeta} + \overline{f}_{,\overline{\zeta}}\dot{\overline{\zeta}})\dot{u} \tag{2.18}$$

But from (2.10)

$$\dot{v} = \frac{1}{U}[\dot{\zeta}\dot{\overline{\zeta}} - \frac{1}{2}(f+\overline{f})U^2 - \frac{\epsilon}{2}] \tag{2.19}$$

We can show (2.18) and (2.19) are consistent equations by differentiating (2.19) with respect to proper time τ, here U$\neq$ 0. For U = 0 the geodesic equations can be simply integrated yielding only trivial null geodesics $\zeta = \zeta_0$, u = u_0, v=$v_1\tau$ +v_0, and spacelike geodesics $\zeta = \frac{1}{\sqrt{2}}\exp(i\phi_0)\tau + \zeta_0$, u = u_0, v = $v_1\tau + v_0$, where ζ_0, u_0, v_1, v_0, and ϕ_0 are constants

$$\ddot{v} = \frac{1}{U}[\ddot{\zeta}\dot{\overline{\zeta}} + \dot{\zeta}\dot{\overline{\zeta}} - \frac{1}{2}(f+\overline{f})_{,u}U^3] \tag{2.20}$$

From (2.15) and (2.16), (2.20) becomes

$$\ddot{v} = \frac{1}{U}[-\frac{1}{2}\overline{f}_{,\overline{\zeta}}U^2\dot{\overline{\zeta}} - \frac{1}{2}f_{,\zeta}U^2\dot{\zeta} - \frac{1}{2}(f+\overline{f})_{,u}U^3]$$

$$\ddot{v} - \frac{1}{2}(f+\overline{f})_{,u}U^2 + (f_{,\zeta}\dot{\zeta} + \overline{f}_{,\overline{\zeta}}\dot{\overline{\zeta}})U = 0 \tag{2.21}$$

Which is identical to (2.18), integrating (2.19), we obtain

$$v(\zeta) - \widetilde{v} = \int \frac{1}{U}[\dot{\zeta}\dot{\overline{\zeta}} - \frac{1}{2}(f+\overline{f})U^2 - \frac{\epsilon}{2}]d\tau \tag{2.22}$$

Re-writing this equation,

$$v(\zeta) = \frac{1}{2U}\int [2\dot{\zeta}\dot{\overline{\zeta}} - (f+\overline{f})U^2 - \epsilon]d\tau + \widetilde{v} \tag{2.23}$$

The three equations (2.15), (2.17), (2.23) appear as geodesic equations of the given metric (2.3), where τ is an affine parameter.

Chapter 3

Chaos in pp-waves

Chaos can appear even in the simplest geodesics motions of non-homogeneous pp-wave space times, with constant profile function. We will show how Hamiltonian flow arises from geodesic equations and the corresponding Hamilton's canonical equations of motions in such space-times. The resultant equations of motion in real coordinates construct a simple system of nonlinear ordinary differential equations (ODE). We will have many higher order systems in the domain of potential function that will appear in Hamiltonian flow. Surprisingly, the corresponding Hamiltonian belongs to a special class of the well-known Hènon-Heiles family where integrability of this family has been under research for four decades. Flow of trajectories in phase-space shows chaotic behaviour. These ODEs seems to have only asymptotic analytic solutions in a global manner.

3.1 Chaotic Hamiltonian Dynamics from Geodesic Equations

In Chapter 2 we introduced the Lagrangian for pp-waves and from it we drived their geodesic equations. From these geodesic equations, in fact it is sufficient to use (2.15) only, we shall find the corresponding Hamiltonian. We give (2.15) again here,

$$\ddot{\zeta} = -\frac{1}{2}\overline{f}_{,\overline{\zeta}}(\dot{u})^2$$

Introducing real coordinates x and y by

$$\zeta = x + iy$$

for non-homogeneous pp-waves f is defined as [9]

$$f = \frac{2}{n} h(u) \zeta^n \tag{3.1}$$

where the parameter n can take constant values n = 3,4,5 ..,

$$d(u) = \frac{2}{n} h(u) = const. \Rightarrow f = C\zeta^n$$

Then (2-15) can be re-written with

$$\begin{aligned} f &= \frac{2}{n} h(u)(x+iy)^n \\ \overline{f} &= \frac{2}{n} h(u)(x-iy)^n \\ \frac{d\overline{f}}{d\overline{\zeta}} &= 2h(u)(x-iy)^{n-1} \end{aligned}$$

Re-arranging (2-15)

$$\frac{d^2(x+iy)}{d\tau^2} + \frac{1}{2} U^2 C n (x-iy)^{n-1} = 0$$

Since this is a complex equation, real and imaginary parts give respectively for n = 3

$$\begin{aligned} \frac{d^2(x+iy)}{d\tau^2} + \frac{1}{2} U^2 C n (x-iy)^2 &= 0 \\ \ddot{x} + \frac{3}{2} U^2 C (x^2 - y^2) &= 0 \\ \ddot{y} - \frac{6}{2} U^2 C x y &= 0 \end{aligned}$$

The equations of motion for n = 3, which will be investigated in the sections that follow, are already in Newtonian form

$$\ddot{x} = y^2 - x^2 \tag{3.2}$$

$$\begin{aligned} \ddot{y} &= 2xy \\ x &= x(\tau), y = y(\tau) \end{aligned} \tag{3.3}$$

The general experession for corresponding Hamiltonian function of the above systems can be written for real cartesian coordinates as

$$H(p_x, p_y, x, y) = H = \frac{1}{2}(p_x^2 + p_y^2) + V(x, y, u) \tag{3.4}$$

where the potential V (this is called an "n-saddle " [7,8]) is defined as

$$V(x, y, u) = \frac{1}{2}U^2 h(u)\,\mathrm{Re}\,(\zeta^n)$$

The shape of this potential function explaining geodesics in corresponding non- homogeneous vacuum pp-wave space-times is shown in figures 3.1, 3.2 and 3.3 for n=3,4,5 respectively.

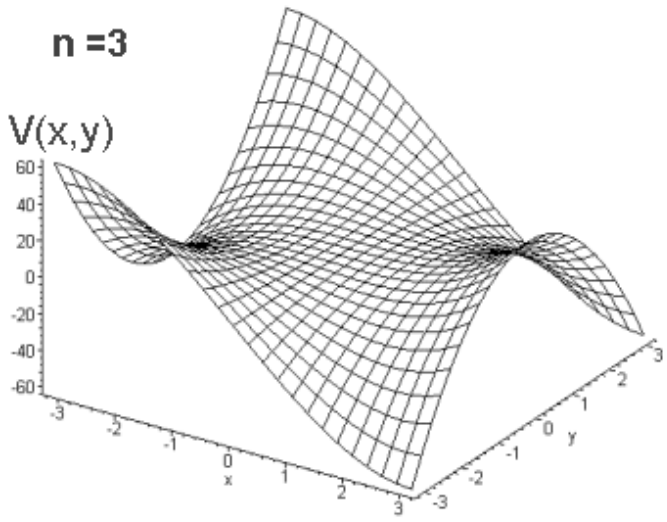

Figure 3-1: The shape of the potential in real-coordinates when parameter n=3 in potential function.

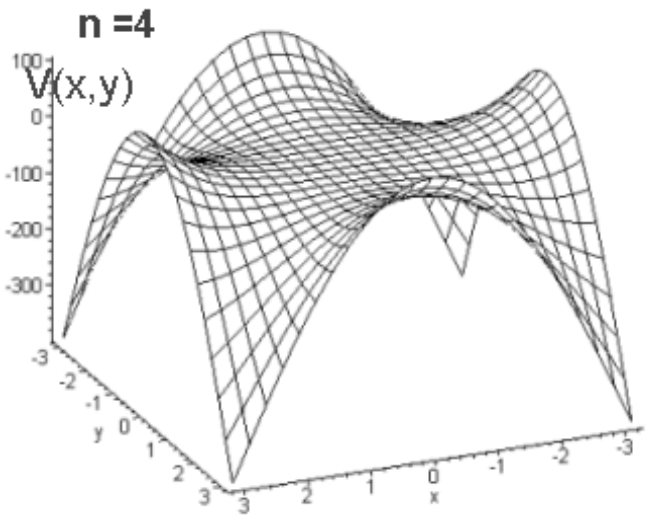

Figure 3-2: The shape of the potential in real-coordinates when parameter n=4 in potential function

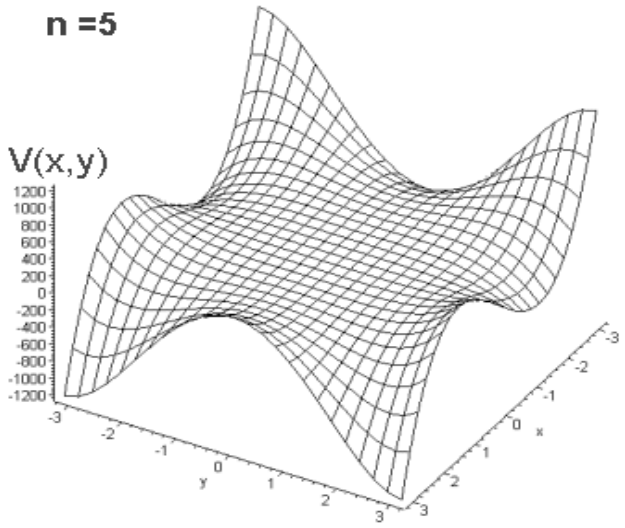

Figure 3-3: The shape of the potential in real-coordinates when parameter n=5 in potential function.

3.2 Hènon-Heiles Hamiltonian

The astronomers Michel Hènon and Carl Heiles worked with different models to understand the motion of stars in the gravitational field of the galaxy, these models are bases for the development and testing of methods of chaotic dynamical systems in pure physics. Even in chemistry same the model was adopted to explain molecular vibrations [4]. The general form of Hènon-Heiles family of Hamiltonian is

$$H(q_1, q_2, p_1, p_2) = \frac{1}{2}(p_1^2 + p_2^2) + \frac{1}{2}(Aq_1^2 + Bq_2^2) + \frac{1}{3}q_1^3 + \lambda q_1 q_2^2 \tag{3.5}$$

where A, B and λ are constant parameters.

In the previous section we have shown the potential function for n=3, simply called the "monkey-saddle" on a plane.[7]

$$V(q_1, q_2) = \frac{1}{3}q_1^3 - q_1 q_2^2 \Longrightarrow V(x, y) = \frac{1}{3}x^3 - xy^2$$

Fascinatingly this potential generates a Hamiltonian that belongs to the Hènon-Heiles family with the following coefficients,

$$A = B = 0, \lambda = -1$$

Integrability of this family was searched for by many researchers, Kowalevskaya and Painlevè analysis which is beyond the scope of this text, show the following cases are realized to be integrable systems in this type of family [4]:

Case 1: $\lambda = 0$ decouples the motion in x and y.

Case2 : $\lambda = -1$ with presence of quadratic terms such as $B = -2, A = 2$ also becomes separable when the coordinates x+y and x-y are used.

Case3: $\lambda = -\frac{1}{6}$ implies the "third" constant of motion could be found

Case4: $\lambda = -\frac{1}{16}$ with $\frac{1}{16}$ coefficient in one of quatratic term is also integrable.

According to the cases above our general Hamiltonian that represents geodesic motion in pp-waves appears to be non-integrable, at least in exact form. Hence it leads to chaos

in geodesic flow due to the system's sensitive dependence on initial condition. That is why the previous section was given the title as chaotic Hamiltonian dynamics. We will investigate numerical and asymtotic solutions in the following sections.

3.3 Numerical Demostration of Chaos in non-homogenous pp-waves

We shall investigate chaos for geodesic motions on a plane space-time for non-homogeneous pp-waves generated by the Hamiltoninan,

$$H(p_x, p_y, x, y) = \frac{1}{2}(p_x^2 + p_y^2) + \mathrm{Re}\,(\zeta^n) \tag{3.6}$$

where $\zeta = x + iy$ and parameter n=3,4,5... . We determine equations of motion for different values of n, using Hamilton's canonical equations, see below. Different potentials have sets of equations having a simple polynomial structure but it is not simple to find exact analytical global solution. Beyond this we needed huge amounts of numerical simulation time to visualize *sensitive dependence on initial conditions* of trajectories.

For comparison of chaotic behaviour with non-chaotic ones we generated geodesics for n=1. This potential leads to an integrable motion and is therefore non-chaotic. Its geodesics are shown in figures 3.4 and 3.5.

3.3.1 Potential Function in the Case of n=2: Homogenous pp-waves

The potential function of the above Hamiltonian represents homogeneous pp-waves in case of n=2. Corresponding geodesic motions are shown in figures 3.6 and 3.7. The geodesic motion are found to be non-chaotic, because, nearby trajectories preserve their separation distance. Liouville's theorem holds for the cases n=1,2. (see figures 3.4, 3.5) In other words, the volume of trajectories are confined into an invariant tori. There is no sensitive dependence on initial conditions. Their equations of motion have an analytical solution and we can predict the motion, hence the Hamiltonian system that generated by homogenous pp-waves is integrable.

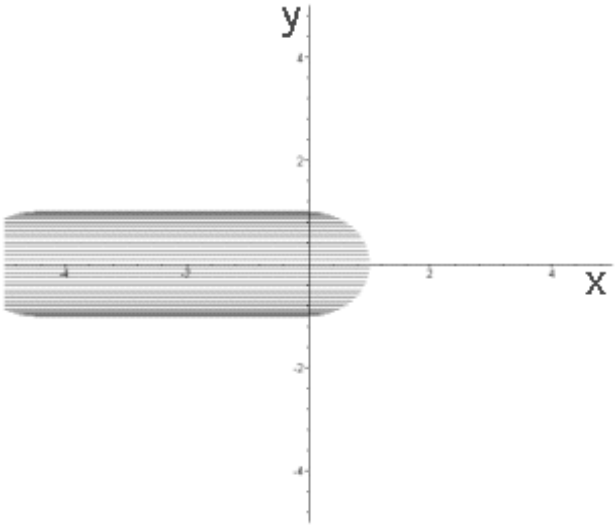

Figure 3-4: Geodesic motions, for n=1 with initial condition from rest with numerical integration of equation of motions.

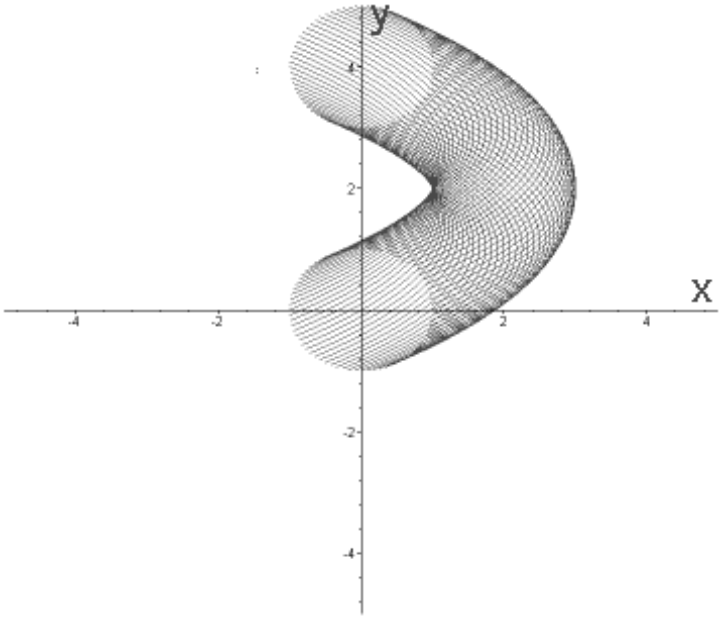

Figure 3-5: Geodesic motions, for n=1 with initial condition.dx/dt=2 and dy/dt=1 with numerical integration of equation of motions.

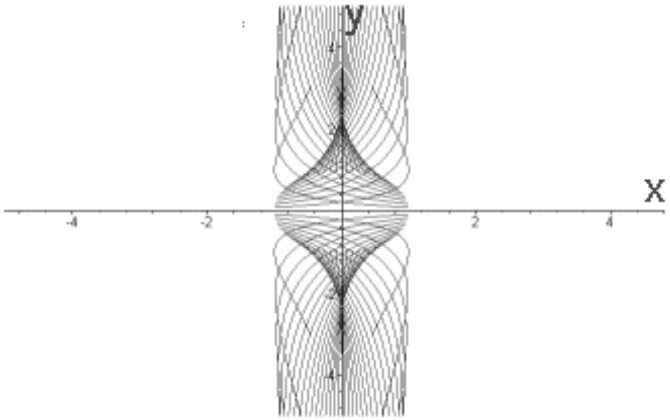

Figure 3-6: Geodesic motions, for n=2 with initial condition from rest with numerical integration of equation of motions.

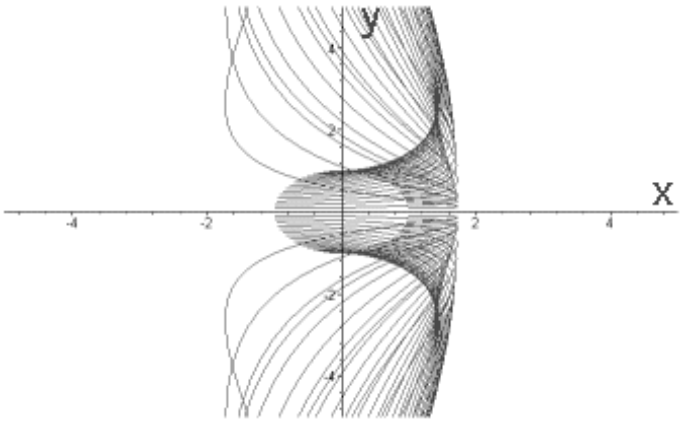

Figure 3-7: Geodesic motions, for n=2 with initial condition.dx/dt=2 and dy/dt=0 with numerical integration of equation of motions.

3.3.2 Polynomial n-saddle Potential Function in the Case of n=3

Potential functions generate different chaotic Hamiltonian systems as we mentioned above Geodesics obtained for n=3 in equation (3.6) are shown figures 3.8-12 with different initial condition; $\dot{x}\ (0) = 0, 2, 3.1, 0$ and $\dot{y}\ (0) = 0, 1, 0.1, 0, 3$ respectively. The phase-spaces are {p_x,x}, {p_y,y} and {p_y,y,x} obtained as in figures 3.14,3.15 and 3.16 respectively.

In figures 3.8-12, we demostrated the behaviour of geodesics with 72 different trajectories with different initial conditions. We can compare them with two different point of views. The first one is in terms if sensitive dependence on initial conditions and the behaviour of nearby trajectories. The second one is distortion of invariant tori and exact analytical solution of equations of motion.

Obviously, trajectories escape along one of the three channels (see figures 3.8 and 3.15), but the density of trajectories is so different for different initial conditions as seen in figures 3.8-12, showing motions are sensitively dependent on initial conditions. In figures 3.9 and 3.10 nearby trajectories diverge exponentially. We would expect symmetric motion in figures 3.11 and 3.12 due to symmetric initial conditions, but due the chaotic behavior of geodesics figures are not symmetric. There is no explicit analytical solution for (3.9-10). There is no smooth invariant torus provided as seen figures 3.13 and 3.14, we could not observe recurrent periodicity in these phase-spaces.

$$H(x,y) = \frac{1}{2}(p_x^2 + p_y^2) + \mathrm{Re}\left((x+iy)^3\right) = \frac{1}{2}(p_x^2 + p_y^2) + \frac{1}{3}x^3 - xy^2$$

$$\frac{dp_x}{dt} = -\frac{\partial H(x,y)}{\partial x} = x^2 - y^2, \frac{dp_y}{dt} = -\frac{\partial H(x,y)}{\partial y} = 2xy \tag{3.7}$$

$$\frac{dx}{dt} = \frac{\partial H(p,q,t)}{\partial p_x} = p_x, \frac{dy}{dt} = \frac{\partial H(p,q,t)}{\partial p_y} = p_y \tag{3.8}$$

$$\ddot{x} = x^2 - y^2 \tag{3.9}$$

$$\ddot{y} = 2xy \tag{3.10}$$

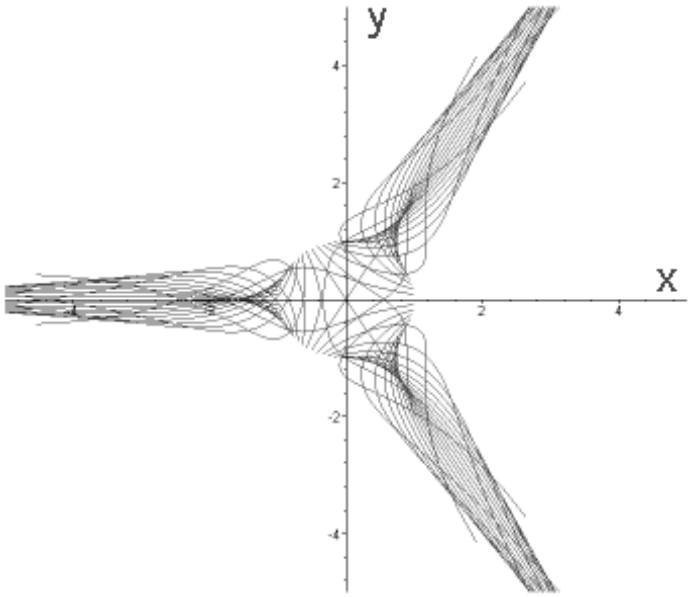

Figure 3-8: Geodesic motions, starting with unit circle, for n=3 from rest, with numerical integration of equation of motions.

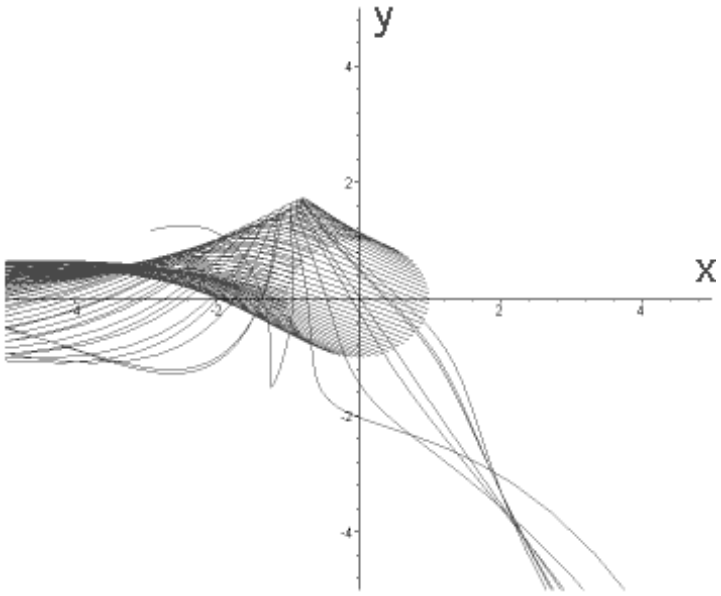

Figure 3-9: Geodesic motions, for n=3 with initial condition, dx/dt=2 and dy/dt=1 with numerical integration of equation of motions.

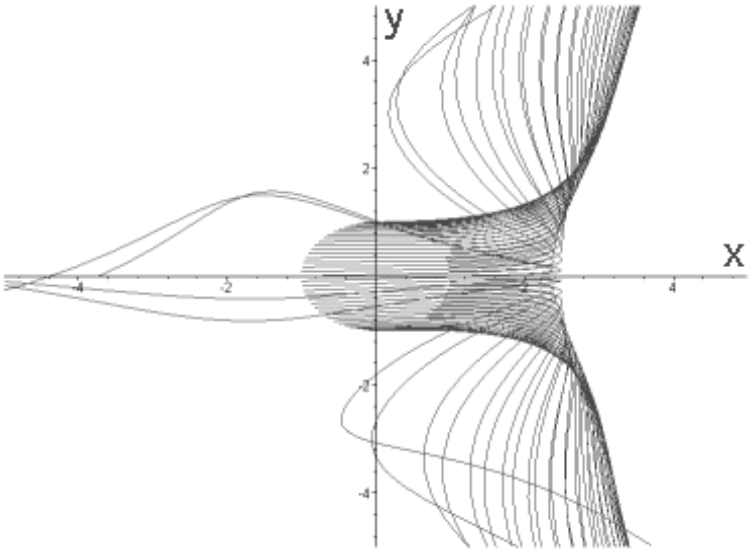

Figure 3-10: Geodesic motions, for n=3 with initial condition.dx/dt=3.1 and dy/dt=0.1 with numerical integration of equation of motions.

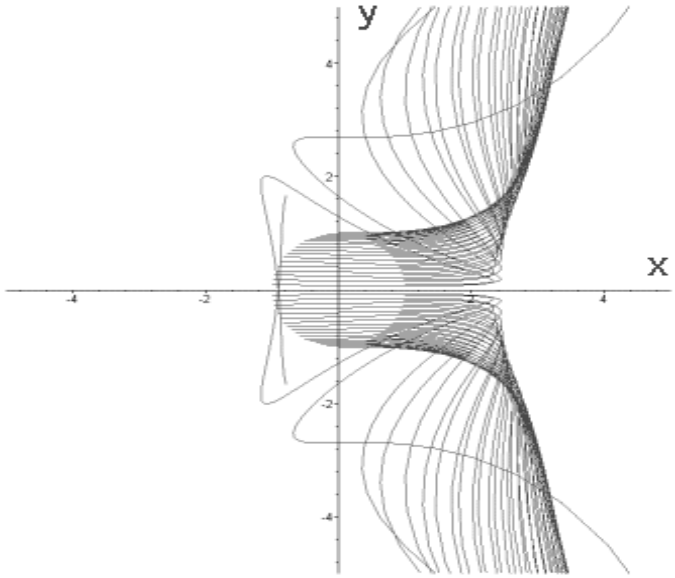

Figure 3-11: Geodesic motions, for n=3 with initial condition. dx/dt=3 and dy/dt=0 with numerical integration of equation of motions.

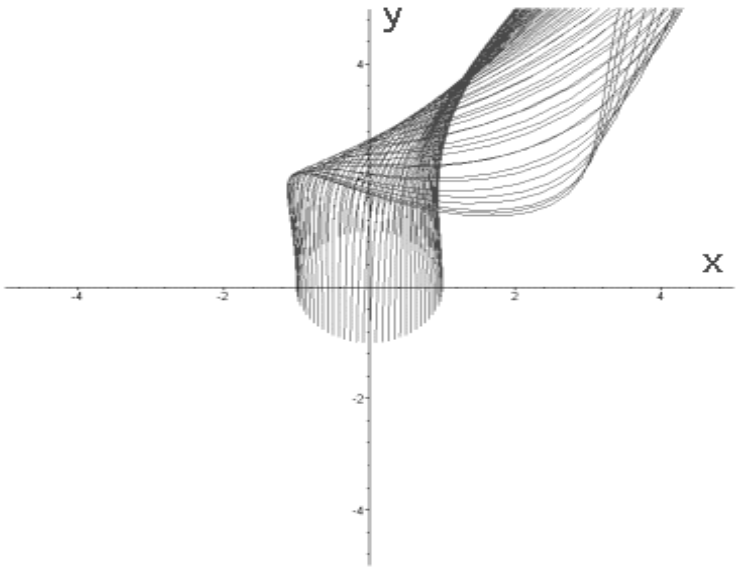

Figure 3-12: Geodesic motions, for n=3 with initial condition dx/dt=0 and dy/dt=3 with numerical integration of equation of motions.

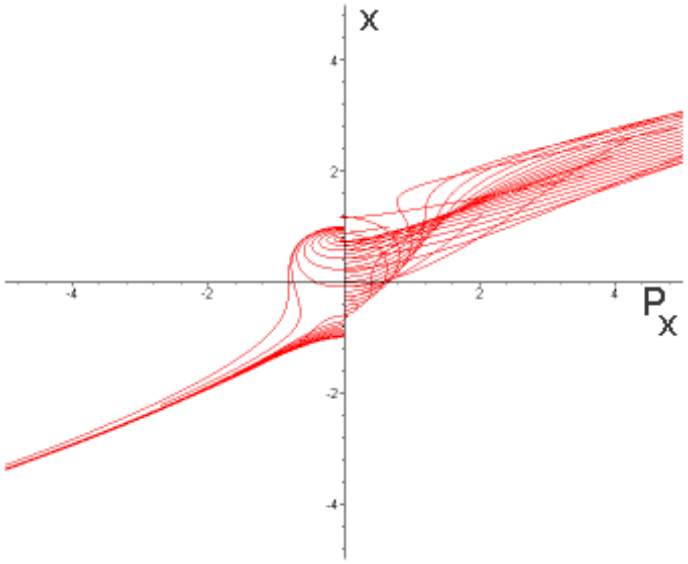

Figure 3-13: Phase-Space $\{P_x, x\}$of the system n=3 from initial condition.dx/dt=0 and dy/dt=0 with numerical integration of equation of motions.

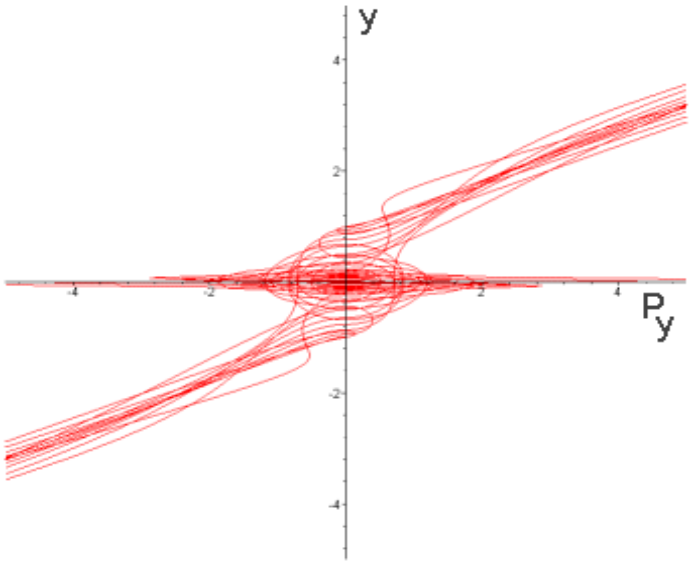

Figure 3-14: Phase-Space $\{P_y, y\}$of the system n=3 from initial condition.dx/dt=0 and dy/dt=0 with numerical integration of equation of motions.

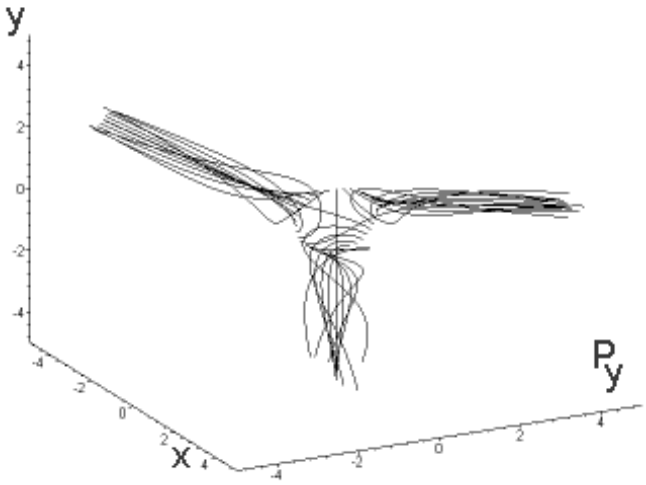

Figure 3-15: Phase-Space $\{P_y, y, x\}$of the system n=3 from initial condition.dx/dt=0 and dy/dt=0 with numerical integration of equation of motions.

3.3.3 Polynomial n-saddle Potential Function in the Case of n=4

We will call the corresponding Hamiltonian, polynomial potential function in real-coordinates for n=4, H_4, and V_4 respectively where dots denotes $\dot{x}= \frac{dx}{dt}$, $\dot{y}= \frac{dy}{dt}$.

$$V_4(x,y) = x^4 - 6x^2y^2 + y^4 \tag{3.11}$$

$$\begin{aligned}
\frac{dp_x}{dt} &= -\frac{\partial H_4(x,y)}{\partial x} = -4x^3 + 12y^2x && (3.12)\\
\frac{dp_y}{dt} &= -\frac{\partial H_4(x,y)}{\partial y} = 12x^2y - 4y^3 && (3.13)\\
\frac{dx}{dt} &= \frac{\partial H_4(p,q,t)}{\partial p_x} = p_x, \frac{dy}{dt} = \frac{\partial H_4(p,q,t)}{\partial p_y} = p_y && (3.14)\\
\ddot{x} &= -4x^3 + 12y^2x, x = x(\tau) && (3.15)\\
\ddot{y} &= 12x^2y - 4y^3, y = y(\tau) && (3.16)
\end{aligned}$$

Geodesics for n=4 are shown in figures 3.16-19 with different initial condition as $\dot{x}\,(0) = 0, 0, 2.5$ and $\dot{y}\,(0) = 0, 2, 0, 4$ respectively. The phase-spaces are $\{p_x,x\}$, $\{p_y,y\}$ and $\{p_y,y,x\}$ similarly in figures 3.20, 3.21 and 3.22 respectively.

In figures 3.16-22, we demostrate the behaviour of geodesics with 72 different trajectories with different initial conditions for n=4. Similar analysis may arise like the one we have done for the case n=3. Four escape channels of geodesics are observed in figures 3.16 and 3.22.

We obtain symmetric motion in figures 3.17 and 3.18 due to symmetric initial conditions, but our potential function is also symmetric. For these reasons, trajectories seems to behave less chaotic, or not strongly chaotic. There is no explicit analytical solution for (3.15-16). There is no smooth invariant torus provided as seen figures 3.20 and 3.21, we could not observe recurrent periodicity in these phase-spaces.

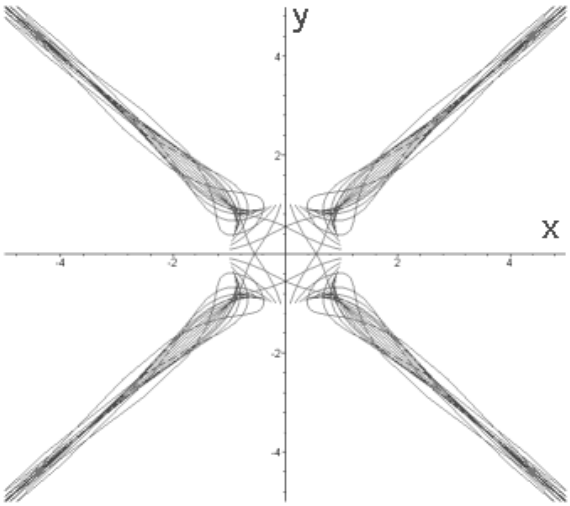

Figure 3-16: Geodesic motions, for n=4 with initial condition.dx/dt=0 and dy/dt=0 with numerical integration of equation of motions.

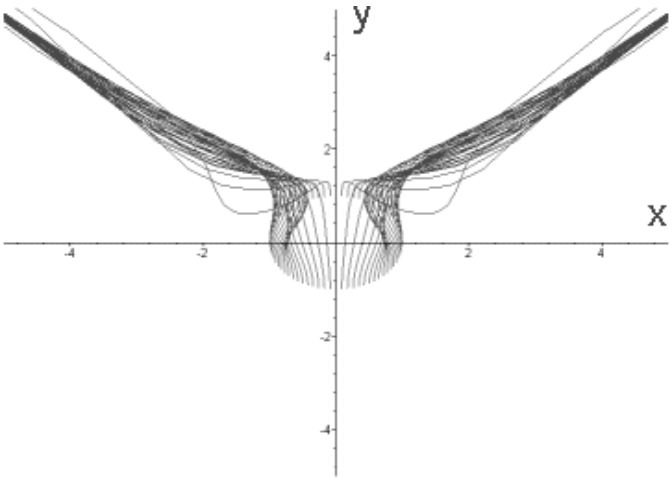

Figure 3-17: Geodesic motions, for n=4 with initial condition.dx/dt=0 and dy/dt=2 with numerical integration of equation of motions.

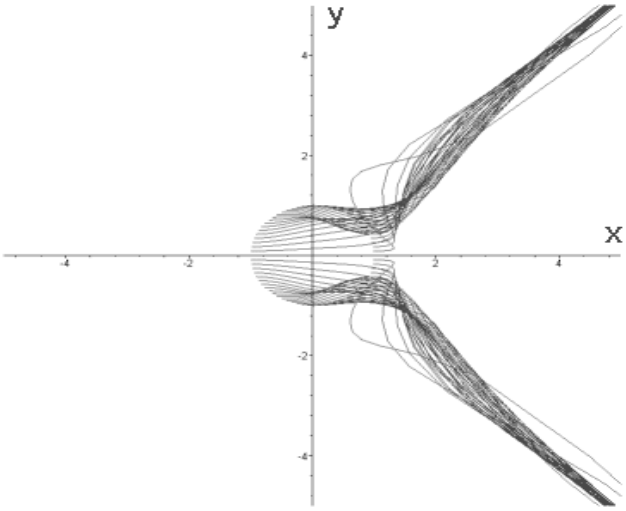

Figure 3-18: Geodesic motions, for n=4 with initial condition.dx/dt=2 and dy/dt=0 with numerical integration of equation of motions.

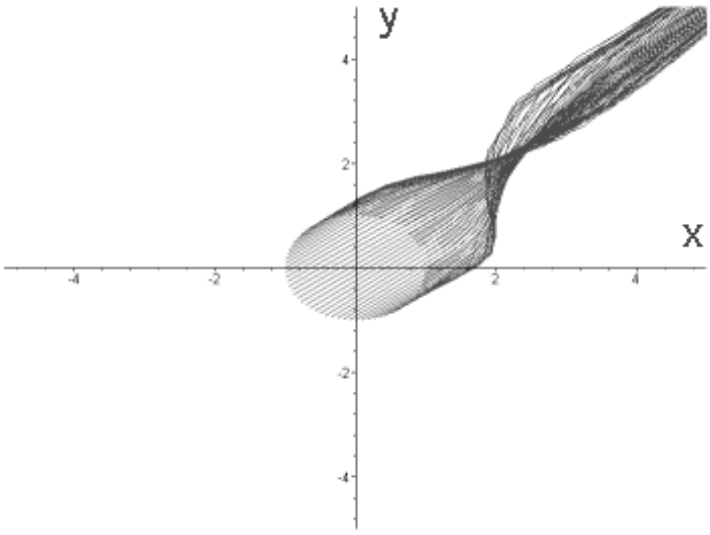

Figure 3-19: Geodesic motions, for n=4 with initial condition.dx/dt=5 and dy/dt=4 with numerical integration of equation of motions.

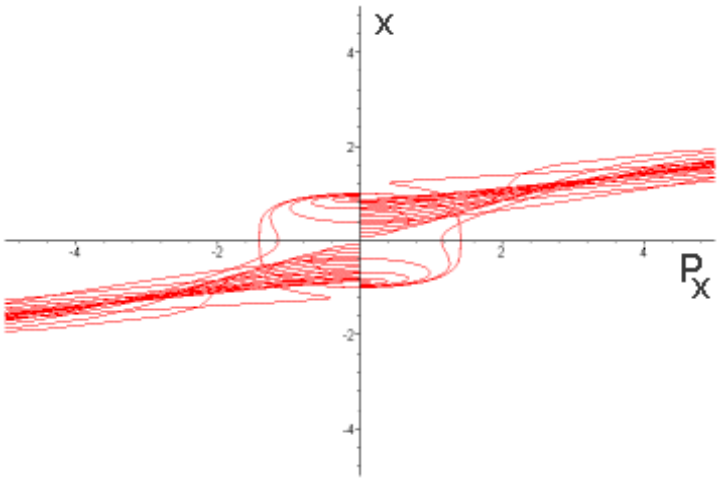

Figure 3-20: Phase-Space $\{P_x, x\}$of the system n=4 from initial condition.dx/dt=0 and dy/dt=0 with numerical integration of equation of motions.

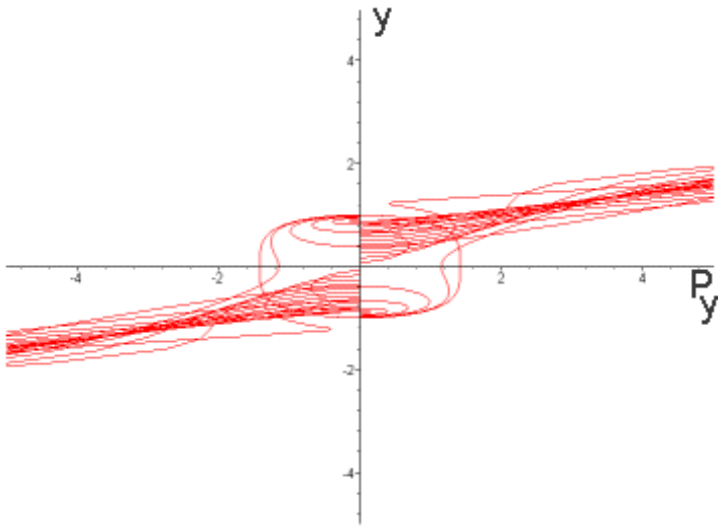

Figure 3-21: Phase-Space $\{P_y, y\}$of the system n=4 from initial condition.dx/dt=0 and dy/dt=0 with numerical integration of equation of motions.

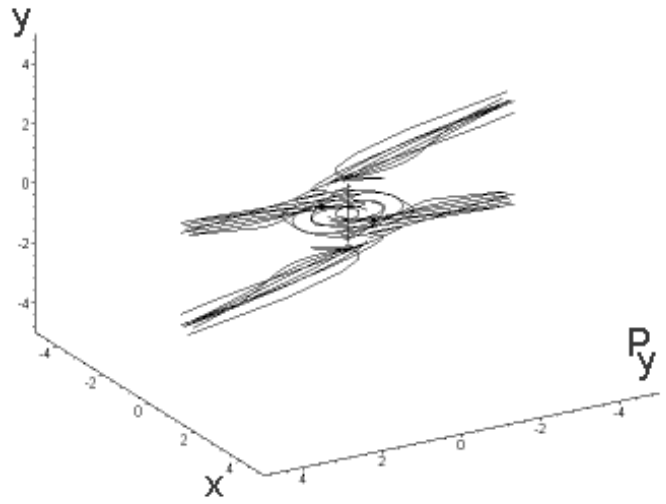

Figure 3-22: Phase-Space $\{P_y, y, x\}$of the system n=4 from initial condition.dx/dt=0 and dy/dt=0 with numerical integration of equation of motions.

3.3.4 Polynomial n-saddle Potential Function in the Case of n=5

We will call the corresponding Hamiltonian, polynomial potential function in real-coordinates for n=5, H_5, and V_5 respectively where dots denotes $\dot{x}= \frac{dx}{dt}$, $\dot{y}= \frac{dy}{dt}$.

$$V_5(x,y) = x^5 - 10x^3y^2 + 5xy^4 \tag{3.17}$$

$$\begin{aligned}
\frac{dp_x}{dt} &= -\frac{\partial H_5(x,y)}{\partial x} = -5y^4 + 30x^2y^2 - 5y^4 && (3.18)\\
\frac{dp_y}{dt} &= -\frac{\partial H_5(x,y)}{\partial y} = 20x^3y - 20x^3y && (3.19)\\
\frac{dx}{dt} &= \frac{\partial H_5(p,q,t)}{\partial p_x} = p_x, \frac{dy}{dt} = \frac{\partial H_5(p,q,t)}{\partial p_y} = p_y && (3.20)\\
\ddot{x} &= -5y^4 + 30x^2y^2 - 5y^4, x = x(\tau) && (3.21)\\
\ddot{y} &= 20x^3y - 20x^3y, y = y(\tau) && (3.22)
\end{aligned}$$

Geodesics for n=5 obtained in figures 3.23-26 with different initial condition $\dot{x}\,(0) =$

$0, 0.9, 2.8, 3.5$ and $\dot{y}\ (0) = 0, 2.1, 1.5, 1.1$ respectively. The phase-spaces are {p_x,x}, {p_y,y} and {p_y,y,x} obtained similarly in figures 3.27, 3.28 and 3.29 respectively.

In figures 3.16-22, we demostrated the behaviour of geodesics with 72 different trajectories with different initial conditions for n=5. Similarly, five escape channels of geodesics are observed in figures 3.23 and 3.29.

Comparison of figures 3.23-28 show that trajectories are sensitively dependent on initial conditions. There is no explicit analytical solution for (3.21-22). There is no smooth invariant torus provided as seen figures 3.20 and 3.21, we could not observe recurrent periodicity in these phase-spaces.

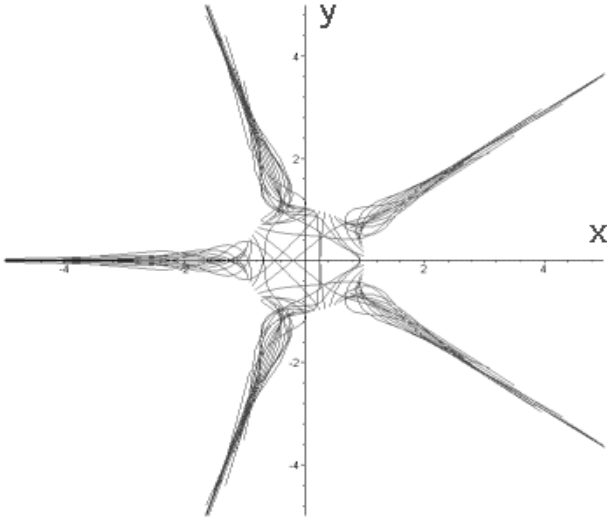

Figure 3-23: Geodesics motion, for n=5 from initial condition.dx/dt=0 and dy/dt=0 with numerical integration of equation of motions.

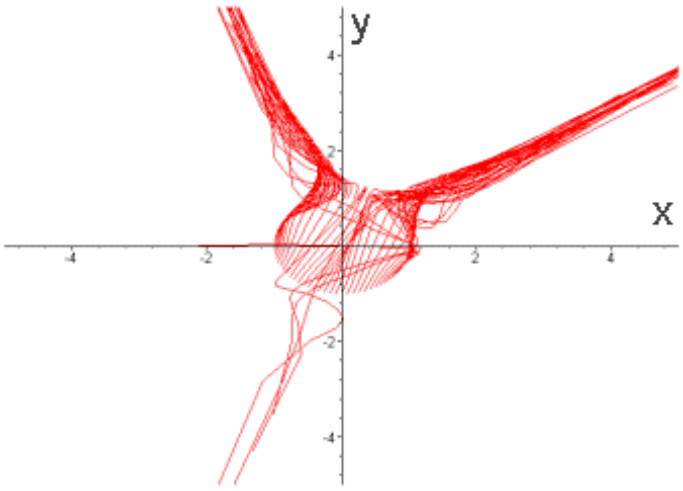

Figure 3-24: Geodesics motion, for n=5 from initial condition.dx/dt=0.9 and dy/dt=2.1 with numerical integration of equation of motions.

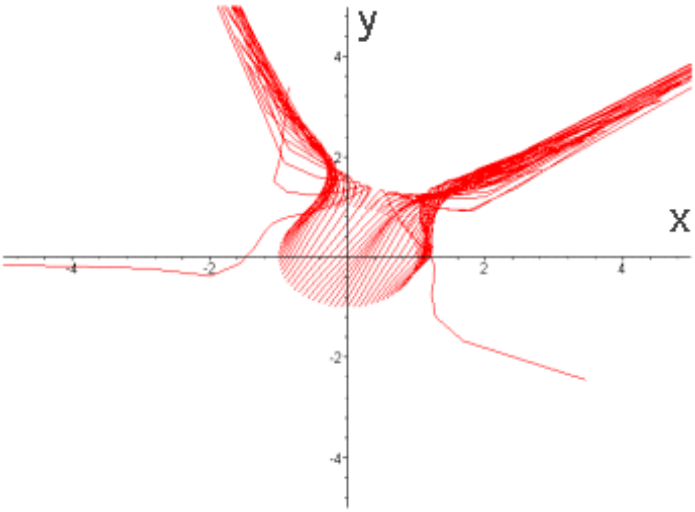

Figure 3-25: Geodesics motion, for n=5 from initial condition.dx/dt=2.8 and dy/dt=1.5 with numerical integration of equation of motions.

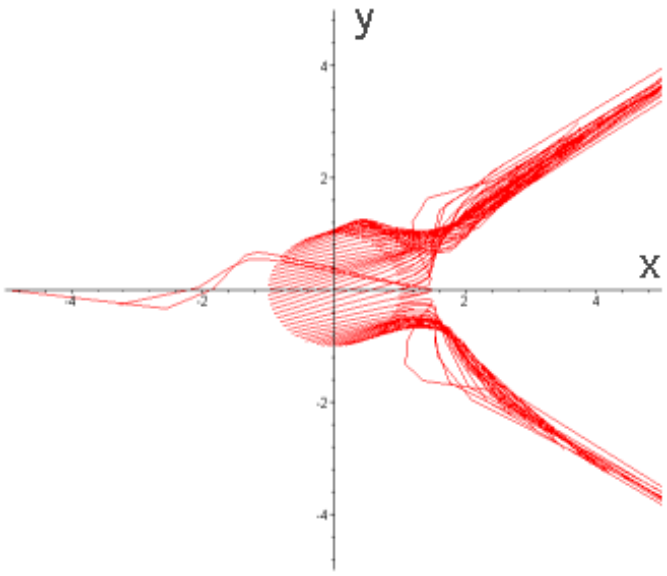

Figure 3-26: Geodesics motion, for n=5 from initial condition.dx/dt=3.5 and dy/dt=1.1 with numerical integration of equation of motions.

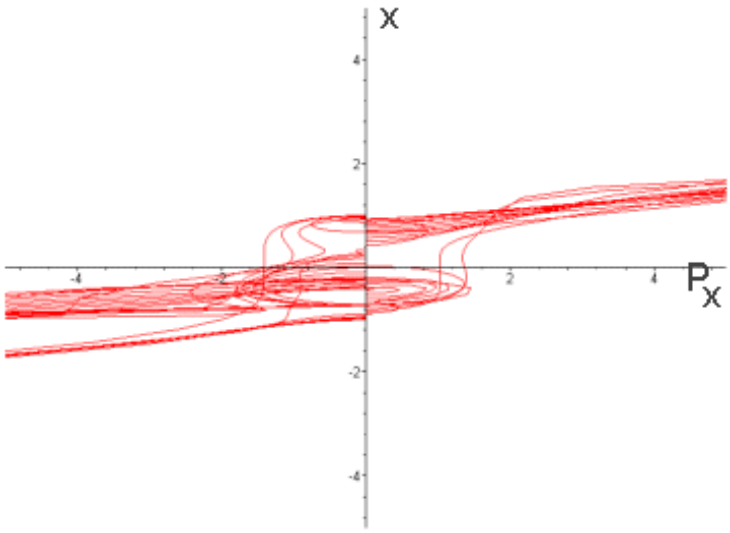

Figure 3-27: Phase-Space $\{P_x, x\}$of the system n=5 from initial condition.dx/dt=0 and dy/dt=0 with numerical integration of equation of motions.

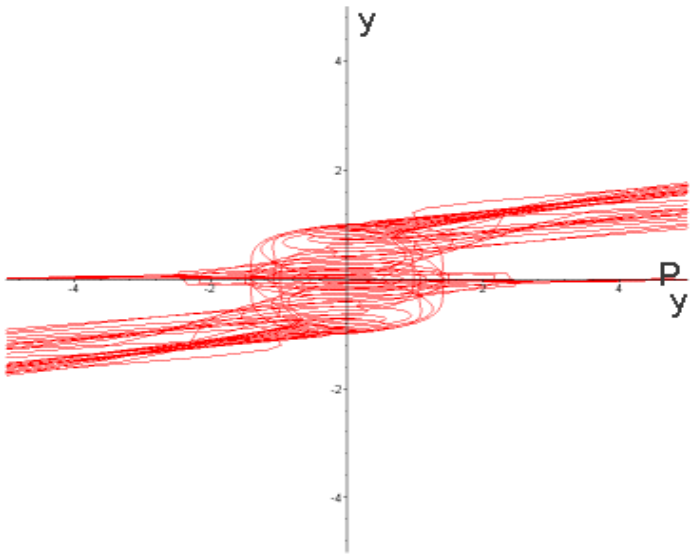

Figure 3-28: Phase-Space $\{P_y, y\}$of the system n=5 from initial condition.dx/dt=0 and dy/dt=0 with numerical integration of equation of motions.

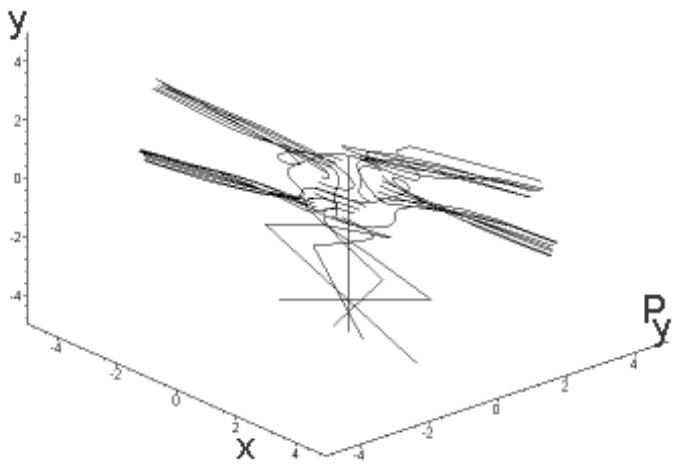

Figure 3-29: Phase-Space $\{P_y, y, x\}$of the system n=5 from initial condition.dx/dt=0 and dy/dt=0 with numerical integration of equation of motions.

3.3.5 Polynomial n-saddle Potential Function in the Case of n=6

We will call the corresponding Hamiltonian, polynomial potential function in real-coordinates for n=6, H_6, and V_6 respectively where dots denotes $\dot{x}= \frac{dx}{dt}$, $\dot{y}= \frac{dy}{dt}$.

$$V_6(x,y) = x^6 - 15x^4y^2 + 15x^2y^4 - y^6 \tag{3.23}$$

$$\begin{aligned}
\frac{dp_x}{dt} &= -\frac{\partial H_6(x,y)}{\partial x} = -6x^5 + 60x^3y^2 - 30xy^4 && (3.24)\\
\frac{dp_y}{dt} &= -\frac{\partial H_6(x,y)}{\partial y} = 30x^4y - 60x^2y^3 + 6y^5 && (3.25)\\
\frac{dx}{dt} &= \frac{\partial H_6(p,q,t)}{\partial p_x} = p_x, \frac{dy}{dt} = \frac{\partial H_6(p,q,t)}{\partial p_y} = p_y && (3.26)\\
\ddot{x} &= -6x^5 + 60x^3y^2 - 30xy^4, x = x(\tau) && (3.27)\\
\ddot{y} &= 30x^4y - 60x^2y^3 + 6y^5, y = y(\tau) && (3.28)
\end{aligned}$$

Geodesics for n=6 obtained in figures 3.30-33 with different initial condition $\dot{x}\ (0) = 0, 2, 3.5, 4$ and $\dot{y}\ (0) = 0, 0.1, 0, 1.2$ respectively. The phase-spaces are $\{p_x,x\}$, $\{p_y,y\}$ and $\{p_y,y,x\}$ obtained similarly in figures 3.34, 3.35 and 3.36 respectively.

In figures 3.30-36, we demostrated the behaviour of geodesics with 72 different trajectories with different initial conditions for n=6. Similarly, six escape channels of geodesics are observed in figures 3.30 and 3.6. And, channels becoming more obvious in phase-spaces.(see figures 3.34-35)

Comparison of figures 3.30-33 show that trajectories are sensitively dependent on initial conditions There is no explicit analytical solution for (3.27-28). There is no smooth invariant torus provided as seen figures 3.20 and 3.21, we could not observe recurrent periodicity in these phase-spaces.

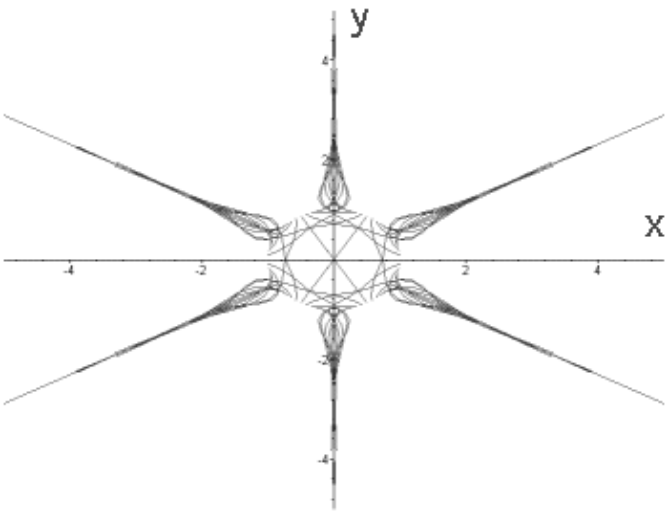

Figure 3-30: Geodesics motion, for n=6 from initial condition.dx/dt=0 and dy/dt=0 with numerical integration of equation of motions.

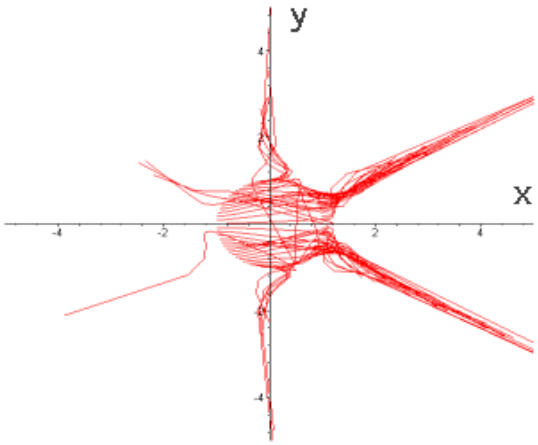

Figure 3-31: Geodesics motion, for n=6 from initial condition.dx/dt=2 and dy/dt=0.1 with numerical integration of equation of motions.

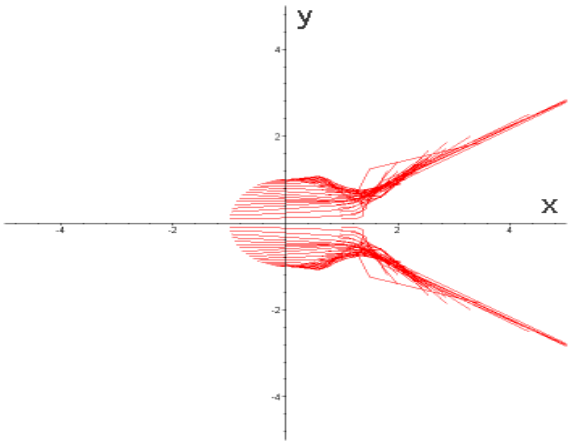

Figure 3-32: Geodesics motion, for n=6 from initial condition.dx/dt=3.5 and dy/dt=0 with numerical integration of equation of motions.

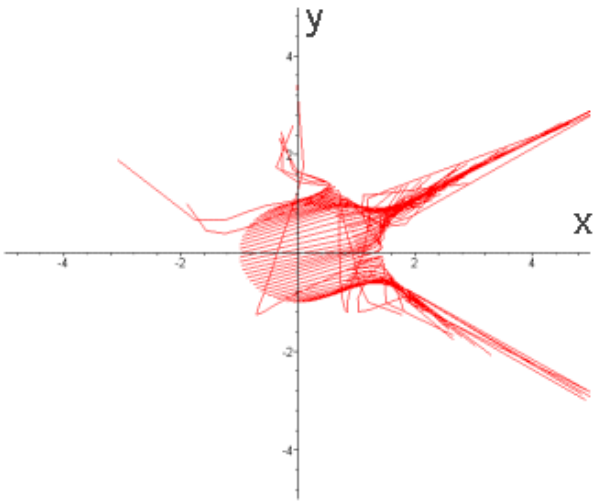

Figure 3-33: Geodesics motion, for n=6 from initial condition.dx/dt=4 and dy/dt=1.2 with numerical integration of equation of motions.

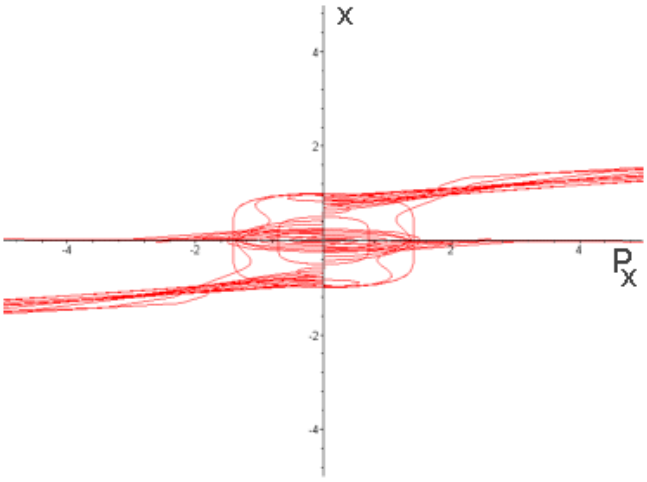

Figure 3-34: Phase-Space $\{P_x, x\}$of the system n=6 from initial condition.dx/dt=0 and dy/dt=0 with numerical integration of equation of motions.

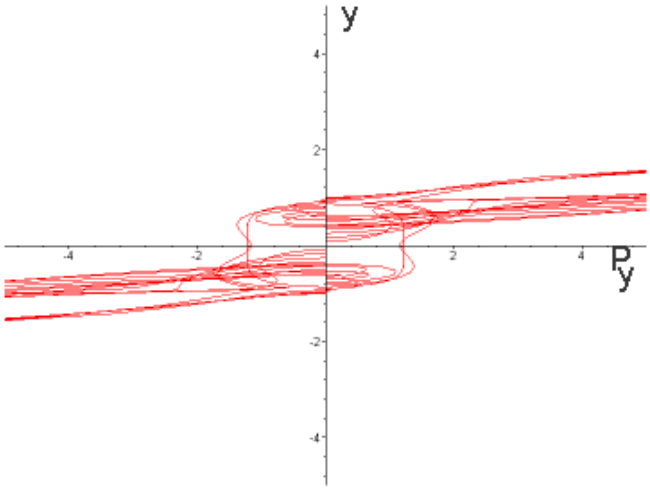

Figure 3-35: Phase-Space $\{P_y, y\}$of the system n=6 from initial condition.dx/dt=0 and dy/dt=0 with numerical integration of equation of motions.

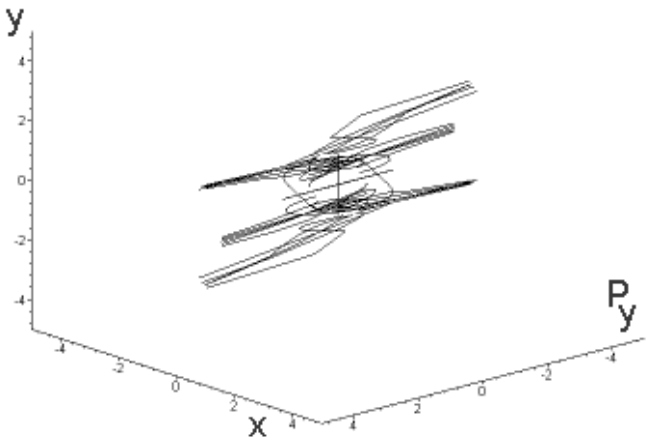

Figure 3-36: Phase-Space $\{P_y, y, x\}$of the system n=6 from initial condition.dx/dt=0 and dy/dt=0 with numerical integration of equation of motions.

3.3.6 Polynomial n-saddle Potential Function in the Case of n=7

We will call the corresponding Hamiltonian, polynomial potential function in real-coordinates for n=7, H_7, and V_7 respectively where dots denotes $\dot{x}= \frac{dx}{dt}$, $\dot{y}= \frac{dy}{dt}$.

$$V_7(x,y) = x^7 - 21x^5y^2 + 35x^3y^4 - 7xy^6 \tag{3.29}$$

$$\begin{aligned}
\frac{dp_x}{dt} &= -\frac{\partial H_7(x,y)}{\partial x} = -7x^6 + 105x^4y^2 - 105x^2y^4 + 7y^6 && (3.30)\\
\frac{dp_y}{dt} &= -\frac{\partial H_7(x,y)}{\partial y} = 42x^5y - 140x^3y^3 + 42xy^5 && (3.31)\\
\frac{dx}{dt} &= \frac{\partial H_7(p,q,t)}{\partial p_x} = p_x, \frac{dy}{dt} = \frac{\partial H_7(p,q,t)}{\partial p_y} = p_y && (3.32)\\
\ddot{x} &= -7x^6 + 105x^4y^2 - 105x^2y^4 + 7y^6, x = x(\tau) && (3.33)\\
\ddot{y} &= 42x^5y - 140x^3y^3 + 42xy^5, y = y(\tau) && (3.34)
\end{aligned}$$

Geodesics for n=7 obtained in figures 3.37-39 with different initial condition $\dot{x}\,(0) = 0, 0, 1.1$ and $\dot{y}\,(0) = 0, 2, 2$ respectively. The phase-spaces are $\{p_x,x\}$, $\{p_y,y\}$ and $\{p_y,y,x\}$ obtained similarly in figures 3.40, 3.41 and 3.42 respectively.

In figures 3.37-42, we demostrated the behaviour of geodesics with 72 different trajectories with different initial conditions for n=7. Similarly, seven escape channels of geodesics are observed in figures 3.37 and 3.42. And, channels are also appear in phase-spaces. (see figures 3.40-41)

Comparison of figures 3.37-39 show that trajectories are sensitively dependent on initial conditions. There is no explicit analytical solution for (3.33-34). There is no smooth invariant torus provided as seen figures 3.40 and 3.41, we could not observe recurrent periodicity in these phase-spaces.

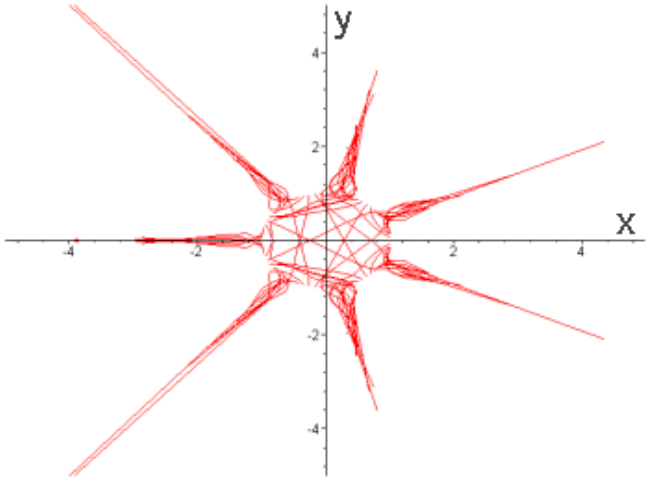

Figure 3-37: Geodesics motion, for n=7 from initial condition.dx/dt=0 and dy/dt=0 with numerical integration of equation of motions.

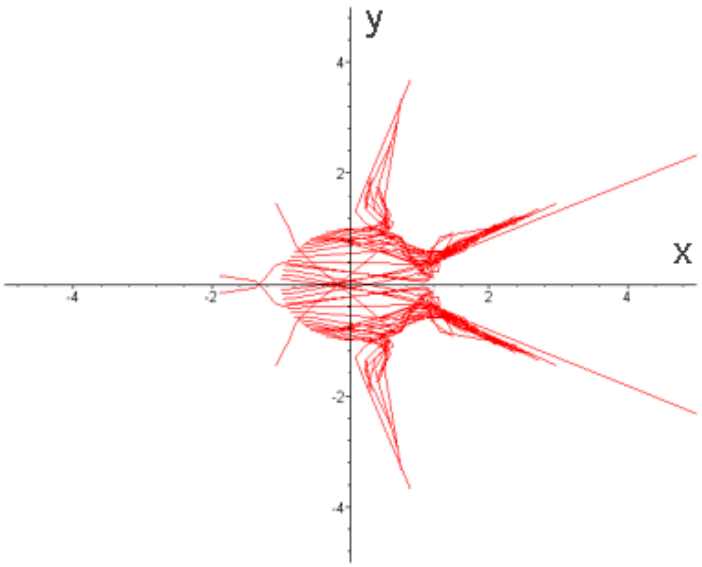

Figure 3-38: Geodesics motion, for n=7 from initial condition.dx/dt=0 and dy/dt=2 with numerical integration of equation of motions.

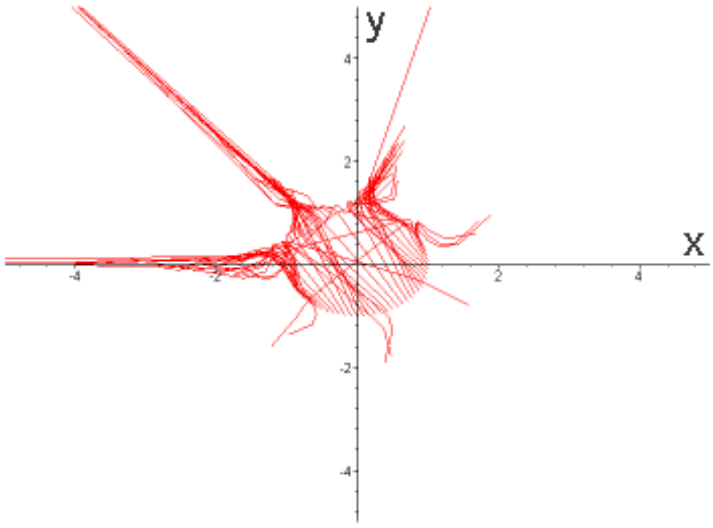

Figure 3-39: Geodesics motion, for n=7 from initial condition.dx/dt=1.1 and dy/dt=2 with numerical integration of equation of motions.

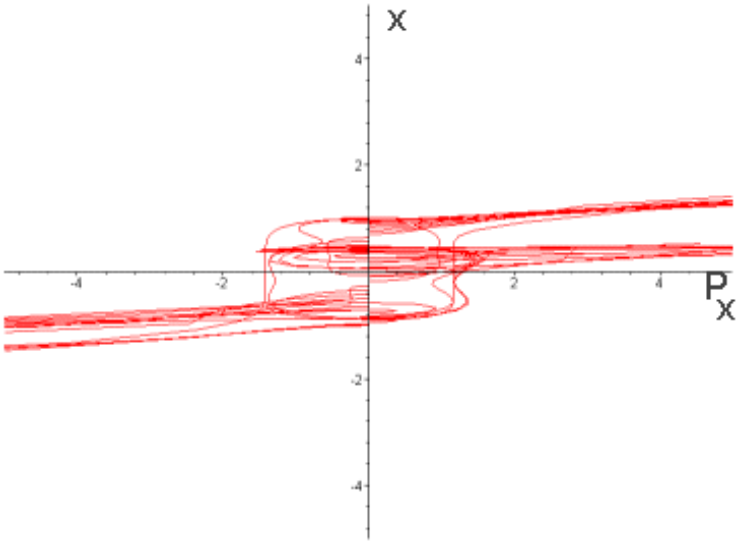

Figure 3-40: Phase-Space $\{P_x, x\}$of the system n=7 from initial condition.dx/dt=0 and dy/dt=0 with numerical integration of equation of motions.

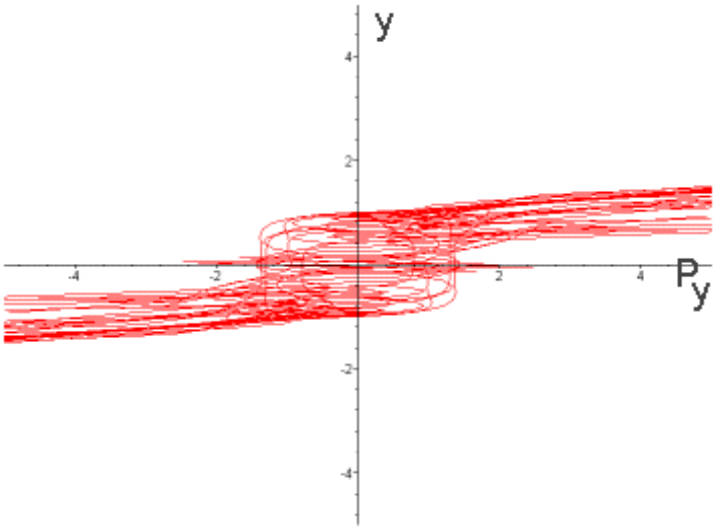

Figure 3-41: Phase-Space $\{P_y, y\}$of the system n=7 from initial condition.dx/dt=0 and dy/dt=0 with numerical integration of equation of motions.

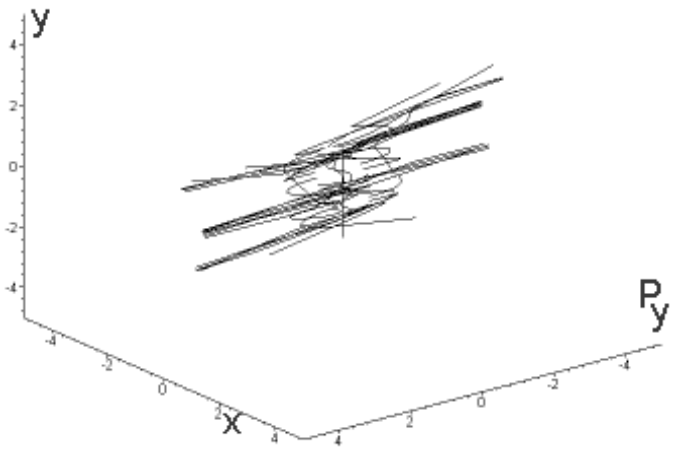

Figure 3-42: Phase-Space $\{P_y, y, x\}$of the system n=7 from initial condition.dx/dt=0 and dy/dt=0 with numerical integration of equation of motions.

We will not do further values of n. Because, the channels that appear in the geodesic motions become too narrower. Making observations for geodesics became harder in this scale.

3.4 Asymptotic Analytic Solution in Polar Coordinates

Non-homogeneous pp-wave space-time generated by the Hamiltonian that we found in (3.4). Let's re-write the potential, and the same Hamiltonian functions [3].

$$\begin{aligned} H(p_x, p_y, x, y) &= H = \frac{1}{2}(p_x^2 + p_y^2) + V(x, y, u) \\ V(x, y, u) &= \frac{1}{2}U^2 h(u)\,\mathrm{Re}\,(\zeta^n), \zeta = x + iy \end{aligned}$$

This potential is called an n-saddle. Transforming to polar coordinates (ρ, ϕ),

$$\begin{aligned} V(\rho, \phi, u_0) &= \frac{1}{n}U^2 h(u_0)\,\mathrm{Re}\,\zeta^n \qquad (3.35) \\ \zeta &= \rho \exp(i\phi) \Rightarrow \zeta^n = \rho^n\{\cos(n\phi) + \sin(n\phi)i\} \\ \mathrm{Re}\,\zeta^n &= \rho^n \cos(n\phi), U^2 h(u_0) = const. = 1 \qquad (3.36) \\ V(\rho, \phi, u_0) &= \frac{1}{n}\rho^n \cos(n\phi) \qquad (3.37) \end{aligned}$$

We have found the conjugate momenta for the new Hamiltonian above where dots denote $\frac{d}{dt}$

$$\begin{aligned} p_x &= \dot{x}, p_y = \dot{y}, x = \rho\cos(\phi), y = \rho\sin(\phi) \\ \dot{x} &= \dot{\rho}\cos(\phi) - \rho\,\dot{\phi}\sin(\phi), \dot{y} = \dot{\rho}\sin(\phi) + \rho\,\dot{\phi}\cos(\phi) \end{aligned}$$

and the new Hamiltonian reduces to

$$\begin{aligned} H(p_\rho, p_\phi, \rho, \phi) &= \frac{1}{2}((\dot{\rho}\cos(\phi) - \rho\,\dot{\phi}\sin(\phi))^2 + (\dot{\rho}\sin(\phi) + \rho\,\dot{\phi}\cos(\phi))^2) + V(\rho, \phi) \\ H(p_\rho, p_\phi, \rho, \phi) &= \frac{1}{2}(\dot{\rho}^2 + \rho^2\,\dot{\phi}^2) + \frac{1}{n}\rho^n\cos(n\phi) \qquad (3.38) \end{aligned}$$

The corresponding Lagrangian can be found from the Legendre transformation

$$\begin{aligned} H(p_\rho, p_\phi, \rho, \phi) &= \dot{\rho}\,\frac{\partial L(\dot{\rho}, \dot{\phi}, \rho, \phi)}{\partial\,\dot{\rho}} + \dot{\phi}\,\frac{\partial L(\dot{\rho}, \dot{\phi}, \rho, \phi)}{\partial\,\dot{\phi}} - L(\dot{\rho}, \dot{\phi}, \rho, \phi) \\ &\Longrightarrow \quad L(\dot{\rho}, \dot{\phi}\,\rho, \phi) = \frac{1}{2}(\dot{\rho}^2 + \rho^2\,\dot{\phi}^2) - \frac{1}{n}\rho^n\cos(n\phi) \end{aligned}$$

$$p_\rho = \frac{\partial L(\dot{\rho},\dot{\phi},\rho,\phi)}{\partial\,\dot{\rho}} = \dot{\rho}, p_\phi = \frac{\partial L(\dot{\rho},\dot{\phi},\rho,\phi)}{\partial\,\dot{\phi}} = \rho^2\,\dot{\phi} \tag{3.39}$$

Equations of motion can be found by using Hamilton's canonical equations as follows

$$\begin{aligned} \dot{p_\rho} &= -\frac{\partial H}{\partial \rho} = -\rho^{n-1}\cos(n\phi) - \rho\,\dot{\phi}^2 \\ \dot{p_\phi} &= -\frac{\partial H}{\partial \phi} = \rho^n \sin(n\phi) \end{aligned} \tag{3.40}$$

Using the relations intoduced above our general expressions for the equations of motion are

$$\ddot{\rho} = -\rho^{n-1}\cos(n\phi) - \rho\,\dot{\phi}^2 \tag{3.41}$$

$$(\rho^2\,\dot{\phi})^{\cdot} = n\rho^n \sin(n\phi) \tag{3.42}$$

These equations are a complicated non-linear second order system of differential equation, and their explicit analytical exact solution seems diffucult to find. For this reason we will employ an asymptotic approximation for the solution of this system of equation.

Any unbounded geodesics escape to infinity only along one of the n channels in the potential. See for example figure 3.8 for n=3. The axes of these outcome channels are given in polar coordinates by the condition [7,8].

$$\cos(n\phi_j) = -1, j = 1, .., n, \sin ce, V \to \infty, \rho \to \infty$$

any unbounded geodesic oscillates around the radial axis ϕ_j of the corresponding jth outcome channel and introduces an equality

$$\begin{aligned} \phi_j &= \frac{(2j-1)\pi}{n} \\ \phi(\tau) &= \Delta\phi_j(\tau) + \phi_j \end{aligned} \tag{3.43}$$

if we choose n=3 then the equations of motion become

$$\ddot{\rho} = -\rho^2\cos(3\phi) - \rho\,\dot{\phi}^2 \tag{3.44}$$

$$(\rho^2\ \dot{\phi})^{\cdot} \quad = \quad 3\rho^3 \sin(3\phi)$$

Determining sine and cosine terms with the equality (3.43)

$$\begin{aligned}
\cos(3\phi) &= \cos 3(\Delta\phi_j(\tau) + \phi_j) = \cos 3\Delta\phi_j(\tau)\cos 3\phi_j - \sin 3\Delta\phi_j(\tau)\sin 3\phi_j \\
\cos(3\phi) &= -\cos 3\Delta\phi_j(\tau) \\
\sin(3\phi) &= \sin 3(\Delta\phi_j(\tau) + \phi_j) = \sin 3\Delta\phi_j(\tau)\cos 3\phi_j - \sin 3\Delta\phi_j(\tau)\cos 3\phi_j \\
\sin(3\phi) &= -\sin 3\Delta\phi_j(\tau) \\
if, [\Delta\phi_j(\tau)]^2 &\approx 0 \Longrightarrow \sin 3\Delta\phi_j(\tau) \approx 3\Delta\phi_j(\tau)
\end{aligned}$$

Let's call $\Delta\phi_j(\tau) = \Psi$ for convenience, then the equations of motion are approximated by

$$\ddot{\rho} \approx -\rho^2 - \rho\ \dot{\Psi}^2 \tag{3.45}$$

$$(\rho^2\ \dot{\Psi})^{\cdot} \approx 3\rho^3\Psi \tag{3.46}$$

even this reduced form is not simple for proceeding with the solution. Making the following anzats seem to solve this system generally,

$$\rho \approx [(n/2-1)\sqrt{CU^2}(\tau_s - \tau)]^{2/(2-n)} \tag{3.47}$$

$$\Psi \approx (\tau_s - \tau)^{\alpha}(A\cos[b\ln(\tau_s - \tau)] + B\sin[b\ln(\tau_s - \tau)]) \tag{3.48}$$

Where A,B,α and b are constants.

3.4.1 Local Solution: In Case of n=3

For n=3 ρ can be expressed with a constant k

$$\rho \approx k(\tau_s - \tau)^{-2} \tag{3.49}$$

Now we attempt to determine the values of α and b,

$$\dot{\rho} \approx -k(\tau_s-\tau)^{-3} \tag{3.50}$$

$$\ddot{\rho} \approx 6k(\tau_s-\tau)^{-4} \tag{3.51}$$

If $\tau_s \to \tau \Longrightarrow \Psi \approx 0$ using (3.45), then

$$\ddot{\rho} \approx -\rho^2$$

$$6k(\tau_s-\tau)^{-4} \approx -k^2(\tau_s-\tau)^{-4} \Longrightarrow k \approx 6$$

we need to determine $\dot{\Psi}$ and $(\rho^2\ \dot{\Psi})^{\cdot}$ hence

$$\begin{aligned}\dot{\Psi} &\approx -\alpha(\tau_s-\tau)^{\alpha-1}(A\cos[b\ln(\tau_s-\tau)] + B\sin[b\ln(\tau_s-\tau)]) \\ &\quad -(\tau_s-\tau)^{\alpha-1}(Bb\cos[b\ln(\tau_s-\tau)] - Ab\sin[b\ln(\tau_s-\tau)]) \\ \dot{\Psi} &\approx -(\tau_s-\tau)^{\alpha-1}\{(A\alpha+bB)\cos[b\ln(\tau_s-\tau)] + (B\alpha-Ab)\sin[b\ln(\tau_s-\tau)]\}\end{aligned} \tag{3.52}$$

$$\rho^2\ \dot{\Psi} \approx -36(\tau_s-\tau)^{\alpha-5}\{(A\alpha+bB)\cos[b\ln(\tau_s-\tau)] + (B\alpha-Ab)\sin[b\ln(\tau_s-\tau)]\} \tag{3.53}$$

With time derivative,

$$\begin{aligned}(\rho^2\ \dot{\Psi})^{\cdot} &\approx 36(\alpha-5)(\tau_s-\tau)^{\alpha-6}\{(A\alpha+bB)\cos[b\ln(\tau_s-\tau)] + (B\alpha-Ab)\sin[b\ln(\tau_s-\tau)]\} \\ &\quad -36(\tau_s-\tau)^{\alpha-6}\{b(A\alpha+bB)\sin[b\ln(\tau_s-\tau)] - b(B\alpha-Ab)\cos[b\ln(\tau_s-\tau)]\} \\ (\rho^2\ \dot{\Psi})^{\cdot} &\approx 36(\tau_s-\tau)^{\alpha-6}\{[(A\alpha+bB)(\alpha-5) + b(B\alpha-Ab)]\cos[b\ln(\tau_s-\tau)] \\ &\quad +[(\alpha-5)(B\alpha-Ab) - b(A\alpha+bB)]\sin[b\ln(\tau_s-\tau)]\}\end{aligned} \tag{3.54}$$

using above equations,

$$(\rho^2\ \dot{\Psi}\ )^{\cdot} \approx 3\rho^3\Psi \approx 3(36)6(\tau_s-\tau)^{\alpha-6}(A\cos[b\ln(\tau_s-\tau)] + B\sin[b\ln(\tau_s-\tau)]) \tag{3.55}$$

$$\approx 36(\tau_s-\tau)^{\alpha-6}\{[(A\alpha+bB)(\alpha-5) + b(B\alpha-Ab)]\cos[b\ln(\tau_s-\tau)] \tag{3.56}$$

$$+[(\alpha-5)(B\alpha-Ab) - b(A\alpha+bB)]\sin[b\ln(\tau_s-\tau)]\} \tag{3.57}$$

The coefficients of the sine and cosine functions should be equal then, combining A and B,

$$-18A \approx (\alpha^2 - 5\alpha - b^2)A + (\alpha b - 5b + \alpha b)B \tag{3.58}$$

$$-18B \approx (\alpha^2 - 5\alpha - b^2)B + (\alpha b - 5b + \alpha b)A \tag{3.59}$$

$$b\alpha - 5b + b\alpha \approx 0 = b(\alpha - 5 + \alpha) \Rightarrow \alpha \approx \frac{5}{2} \tag{3.60}$$

$$\alpha^2 - 5\alpha - b^2 + 18 \approx 0 \Rightarrow b \approx \frac{\sqrt{47}}{2} \tag{3.61}$$

these are local values of α and b.

3.4.2 Global Solution: In General Case

We obtained asymptotic geodesic equations as approximate solution in equations (3.45-3.46). In the general case.

$$\ddot{\rho} \approx -\rho^{n-1} - \rho\,\dot{\Psi}^2$$

$$(\rho^2\,\dot{\Psi})^{\cdot} \approx n\rho^n\Psi$$

We can introduce following anzats

$$\rho \approx k(\tau_s - \tau)^{\frac{2}{2-n}} \tag{3.62}$$

$$\Psi \approx (\tau_s - \tau)^{\alpha}(A\cos[b\ln(\tau_s - \tau)] + B\sin[b\ln(\tau_s - \tau)]) \tag{3.63}$$

derivatives of these functions appear as expressions in the geodesic equations as

$$\begin{aligned}
\dot{\Psi} &\approx -\alpha(\tau_s - \tau)^{\alpha-1}(A\cos[b\ln(\tau_s - \tau)] + B\sin[b\ln(\tau_s - \tau)]) \\
&\quad -(\tau_s - \tau)^{\alpha-1}(-bA\sin[b\ln(\tau_s - \tau)] + Bb\cos[b\ln(\tau_s - \tau)]) \\
\dot{\Psi} &\approx (\tau_s - \tau)^{\alpha-1}\{(-Bb - \alpha A)\cos[b\ln(\tau_s - \tau)] + (bA - \alpha B)\sin[b\ln(\tau_s - \tau)]\} \\
\rho^2\,\dot{\Psi} &\approx k^2(\tau_s - \tau)^{\frac{4}{2-n}+\alpha-1}\{(-Bb - \alpha A)\cos[b\ln(\tau_s - \tau)] + (bA - \alpha B)\sin[b\ln(\tau_s - \tau)]\} \\
(\rho^2\,\dot{\Psi})^{\cdot} &\approx -k^2(\frac{4}{2-n} + \alpha - 1)(\tau_s - \tau)^{\frac{4}{2-n}+\alpha-2}
\end{aligned}$$

$$
\begin{aligned}
&\{(-Bb-\alpha A)\cos[b\ln(\tau_s-\tau)]+(bA-\alpha B)\sin[b\ln(\tau_s-\tau)]\}\\
&-bk^2(\frac{4}{2-n}+\alpha-2)(\tau_s-\tau)^{\frac{4}{2-n}+\alpha-2}\\
&\{(Bb+\alpha A)\sin[b\ln(\tau_s-\tau)]+(bA-\alpha B)\cos[b\ln(\tau_s-\tau)]\}\\
\approx\ & nk^n(\tau_s-\tau)^{\frac{2n}{2-n}+\alpha}(A\cos[b\ln(\tau_s-\tau)]+B\sin[b\ln(\tau_s-\tau)])
\end{aligned}
$$

since powers of $(\tau_s-\tau)$ are equal in both sides, then

$$
\begin{aligned}
(\rho^2\ \dot{\Psi})^{\cdot} &\approx k^2\{[(\frac{4}{2-n}+\alpha-1)(Bb+\alpha A)+b(\alpha B-bA)]\cos[b\ln(\tau_s-\tau)]\\
&\quad+[(\frac{4}{2-n}+\alpha-1)(-bA+\alpha B)-b(\alpha A+bB)]\sin[b\ln(\tau_s-\tau)]\}\\
&\approx nk^n(A\cos[b\ln(\tau_s-\tau)]+B\sin[b\ln(\tau_s-\tau)])
\end{aligned}
$$

coefficients of sine and cosine functions should be equal then,

$$
\begin{aligned}
nk^{n-2}A &\approx \{(\frac{4}{2-n}+\alpha-1)(Bb+\alpha A)+b(\alpha B-bA)\}\\
nk^{n-2}B &\approx \{(\frac{4}{2-n}+\alpha-1)(-bA+\alpha B)-b(\alpha A+bB)\}
\end{aligned}
$$

combining A and B,

$$
\begin{aligned}
nk^{n-2}-(\frac{4}{2-n}+\alpha-1)\alpha+b^2 &= 0\\
(\frac{4}{2-n}+\alpha-1)b+\alpha b &= 0\Rightarrow\alpha=\frac{1}{2}\frac{n+2}{n-2} \qquad (3.64)\\
nk^{n-2}-(\frac{4}{2-n}+\frac{1}{2}\frac{n+2}{n-2}-1)\frac{1}{2}\frac{n+2}{n-2}+b^2 &= 0\\
b^2+nk^{n-2}-\alpha^2 &= 0\\
\frac{2n^2}{(n-2)^2}-\frac{1}{4}\frac{(n+2)^2}{(n-2)} &= b^2\Longleftrightarrow k^{n-2}=\frac{-2n}{(n-2)^2}\\
\frac{1}{2(n-2)}\sqrt{8n^2-(n+2)^2} &= b\Rightarrow b=\frac{1}{2(n-2)}\sqrt{7n^2-4n-4} \qquad (3.65)
\end{aligned}
$$

constants α and b are expressed in terms of n that appears in structural function ζ in metric of pp-waves, which is critical for the derivation of corresponding Hamiltonian and geodesic equations. We demostrate that these equations have asymtotical solutions as approximation.

Chapter 4

Conclusions

Physical systems that obey classical mechanics address the problem of integrability. Many times we employ concepts such as integrability, predictibility and determinisim without care in standard mechanics [3]. Combination of non-integrability, determinism and unpredictibility in the dynamical evolution of certain physical systems even ones as very simple and well-known as pp-waves, can be complex [7,8,9,12]. We introduced the term "Hamiltonian Deterministic Chaotic Dynamics" for this type of system.

In our work an example of a member of the well-known Hènon-Heiles (HH) Hamiltonian family suprisingly was derived from the metric of a free test particle that describes homogeneuos (quadratic structural function ζ^2) and non-homogeneous (structural function ζ^n n $\geq$ 3) vacuum plane fronted gravitational waves in Minkowski space-times which are the simplest waves in the theory of General Relativity. We established all types of geodesics: timelike, null and spacelike.

Our discussion started in a historical manner: in brief, from the birth of classical mechanics and its main evolution to chaos with mathematical origins [4]. Dynamics of planar flow and Poincarè sectioning of HH system were obtained by numerical techniques which has well-founded theoretical basis. Geodesics in pp-waves start from the definition of a metric found by Brinkmann, and derivation of geodesic equations by standard methods of classical mechanics with simple relativistic approach. And corresponding Hamilton's canonical equations were obtained. We also confirmed our results with algebraic computation packages.

We investigated the space-times of pp-waves with the function f(ζ^n) of the simplest form f $\sim \zeta^n$ as profile function h(u)→constant in detail, for n=2 homogeneous pp-waves and n=3,4,5,6,7 non-homogeneous pp-waves. For non-constant profile function cases studied in the reference [9] as sandwich pp-waves. Our observations from our massive numerical and asymtotic analytical solutions are as follows ;

- Quadratic structural function ζ^2, generates integrable and non-chaotic regular Hamiltonian motion. There is no sensitive dependence on initial conditions. Evolution of nearby trajectories remains the same in terms of seperation of geodesic motions. Decision of escape channels by test particles are predictable.

- For cubic (n=3) and other cases (n=4,5,6,7) the metric of pp-waves generates non-integrable and chaotic irregular Hamiltonian motion. There is "sensitive dependence on initial conditions", as seen in generated figures 3.4 to 3.42. Evolution of nearby trajectories exponential fashion in terms of separation of geodesic motions. Decision of escape channels by test particles are unpredictable in long term.

- Our numerical simulations demostrated that, compututon time increases when we increase the number of channels, this is the signature of "increasing complexity", it appears to be another definition of chaos.

- Phase-spaces of each number of channels as conjugate momenta versus position show from a different point of view that the above statements are correct.

- If we compare these chaotic phase spaces with the phase-space of simple harmonic oscillation, irregularities appears very obviously.

- In our asymptotic solutions in polar coordinates, we obtained exact expressions for solutions. These solutions imply that the behaviour of geodesics in pp-waves are asymtotically integrable.

- Our attempt to solve the geodesic equation in polar coordinates (even for local n=3) in a general sense by the very powerful algebraic packages and computers is of no use. This is a signature of increasing complexity.

The study of chaotic and highly nonlinear systems is still expanding and is an active research topic in contemporary theoretical physics, as in General Relativity where the nature of this theory is strongly nonlinear [7]. Chaotic dynamics in gravitational waves has already appeared as a current and promising research field, as an extention of cosmological and astrophysical context. A deeper cutting edge topic called "Quantum Chaos" [4], where quantum analogies of chaotic or quantization of non-integrable systems are under investigation by a semi-classical approach, is important due to fundamental problems of physics such as correpondence between micro and macro world. Even applied and experimental physics have employed well founded chaotic dynamical tools, that were imported from applied mathematics, and it is becoming a growing industry. Also, investigation of connections of chaos theory with fields such as statistical mechanics, quantum computing has become hot topics.

Chapter 5

Appendices

5.1 MapleV Source Codes

5.1.1 Hènon-Heiles Poincarè-mapping

```
# Poincare Sectioning of particular example of Henon-Heiles Family
# Refreshing memory, and calling differential equations packages.
> restart:with(DEtools,poincare,generate_ic,zoom,hamilton_eqs);
# Definition of our Hamiltoninan
> H := 1/2*(p1^2+p2^2+q1^2+q2^2)+q1^2*q2-q2^3/3;
# Generating initial conditions for each constant energy surfaces
# as 1/24,1/18,1/12,1/8,1/7,1/6, loop defined
> for h in [1/24,1/18,1/12,1/8,1/7,1/6] do
> ics[h] := generate_ic(H,{t=0,p2=0.1,q2=-0.2..0.2,q1=-0.2..-0.1,energy=h},3)
> od;
# Numerical calculation of each surface sections
>for h in [1/24,1/18,1/12,1/8,1/7,1/6] do F4[h] := poincare(H,t=-300..300,ics[h],
> stepsize=.1,iterations=3,scene=[p2=-.5..0.5,q2=-.5..0.5]):
> od:
# Plotting the numerical sets that obtained above.
>FF4 := array([[F4[1/24],F4[1/18],F4[1/12]],[F4[1/8],F4[1/7],F4[1/6]]])
```

```
>plots[display](FF4);
# sections displayed.
```

5.1.2 Hamilton Equations : N-Saddle Hamiltonians

```
> restart:
# Refreshing memory
> with(plots):with(DEtools):
# Calling Package for plot structure and differential equations.
# Hamiltonian sub-package imported.
# Defining Monkey Saddle Hamiltonian with potential function.
> H:=1/2*(p1^2+p2^2)+V(q1,q2);
# We need to find different outcames arising from parameter
# that appear in potetial as n, loop defined.
> for n from 1 to 7 do
> V[n]:=evalc(Re((q1+I*q2)^n)):
> H[n]:=1/2*(p1^2+p2^2)+V[n];
> hamilton_eqs(H[n]);
> od;
# Equations of gedesics obtained.
```

5.1.3 Visualisation of Geodesic Motion

```
# Numerical Demostration of the solution of Hamiltonian motion
# in cartesian coordinates for particular case of n=3 in potential function.
# Clear the memory.Calling packages for differential equations and
# plotUtilities.
> restart:with(DEtools):with(plots):
# Solution of Hamilton equations for the particular case n=3
# As a second order nonlinear ordinary differential equation
# Equation set and initial conditions defined as
> de1 := {(D@@2)(x)(t)=y(t)^2-x(t)^2, (D@@2)(y)(t)=2*x(t)*y(t)}:
```

```
> init1 := {x(0)=0, D(x)(0)=0, y(0)=1, D(y)(0)=0}:
# Solving these equations by Numerical Method
# RUNGE-KUTTA-FEHLBERG Method (RFK45)
> F := dsolve(de1 union init1, {x(t),y(t)},type=numeric);
# Construction of loop for great number of trajectories
# starting from unit circle and displaying plots in one graphic
> for k from 0 to 71 do
> init[k]:= {x(0) = cos(k*2*Pi/72), y(0) = sin(k*2*Pi/72), D(x)(0)=0,
> D(y)(0) = 0};
> F[k]:= dsolve(de1 union init[k], {x(t),y(t)},type=numeric);
> P[k]:= odeplot(F[k],[x(t),y(t)],0..4);
> od:
> display({seq(P[k],k=0..71)},view=[-5..5,-5..5]);
# If we changed equations for various type of potentials and initial
# conditions, geodesic flows could be investigated as in figures given above.
```

Chapter 6

References

[1] Tufillaro, Abbott, Reilly, An Experimental Approach to Nonlinear Dynamics and Chaos.(Addison Wesley, 1992)

[2] Gutzwiller C. Martin ,Progress of Theoretical Physics Supplement No.116, 1994

[3] Herbert Goldstein, Classical Mechanics Second Edition(Addison Wesley, New York 1980)

[4] Gutzwiller C. Martin , Chaos in Classical and Quantum Mechanics (Springer -Verlag New York,Heidelberg,Berlin 1990)

[5] Ferdinand Verhulst , Nonlinear Differential Equations and Dynamical Systems (Springer-Verlag Berlin Heidelberg 1990 1996)

[6] J. Guckenheimer and P.Holmes, Nonlinear Oscillations, dynamical systems and Bifurcation of vector fields. (Springer -Verlag New York„Heidelberg,Berlin 1983)

[7] J. Podolsky and K. Vasely, Physical Rewiev D.Volume 58. 081501

[8] J. Podolsky and K. Vasely, pre-print gr-qc/9809065

[9] J. Podolsky and K. Vasely,Class. Quantum Grav. 16 (1999) 3599-3618

[10] J.W. van Holten, Gravitational Waves and Black Holes, pre-print gr-qc/9704043

[11] Bjorn Felsager, Geometry, Particles and Fields (Springer -Verlag New York,Heidelberg,Berlin 1998)

[12] J. Podolsky and K. Vasely, pre-print gr-qc/0006066

Chapter 7

Acknowledgements

I was lucky to have the opportinity of attending Professor Mustafa HALILSOY's lectures on classical mechanics as a basic background of this thesis. I would like to extend my sincere thanks to him for working under his supervision, his guidance, his humanity and his deep physics knowledge.

I would like to extend my sincere thanks to my brother Ziya Suzen, my parents whose never ending love and encrougements, their endless support during my study with their vision of life.

Special thanks to Dr.Armin Kargol and Dr.Eser Aydiroglu for their supervision in my first year. I would like to thank Halil Berberoglu for editing the text.

Many thanks to Dr.Podolsky Jiri for his comments on my numerical algorithms, Prof.Dr.R.C. Churchill, and Prof.Dr.D.L. Rod providing us their theory publications.

Also thanks to Izzet, Erinc, Ali, Raif, Sadik, Ibrahim, Hale, Hamide and Sonuc for their friendship and Maen Odeh for his conversation about fundamentals of Physics and life.

And finally, thanks to the Department of Physics for providing me this source of teaching and learning environment for two years of my MS study.

ABSTRACT

THE CHAOTIC BEHAVIOUR OF GEODESICS IN NON-HOMOGENEOUS VACUUM pp-WAVE SOLUTIONS

Master of Science in Physics

Mehmet Ali SUZEN

Supervisor : Prof. Dr. Mustafa HALILSOY

59 pages, 18 September 2000

We demostrate chaotic behaviour of time-like, space-like and null geodesics of a free test particle in non-homogeneous vacuum plane fronted gravitational waves with asymptotic analytical and numerical methods. Geodesic motions that we derived from the pp-wave metric, generate deterministic chaotic Hamiltonian flow on a plane of real coordinates and corresponding phase-spaces in the case of $n \geq 3$, which belongs to the famous Hénon-Heiles family. Analyzing integrability of this type of Hamiltonian flow shows that even simple and well-know dynamics of pp-waves could evolve in complex fashion.

ÖZET

BOSLUKTA YAYILAN- HOMOJEN OLMAYAN DUZLEMSEL DALGA GEODEZIKLERININ KAOTIK DAVRANISLARI

Fizik Master Tezi

Mehmet Ali SUZEN

Tez Danismani : Prof. Dr. Mustafa HALILSOY

59 sayfa, 18 Eylul 2000

Etkilesimsiz test parcaciklarinin zamansal, uzaysal ve isiksal geodeziklerinin homojen olmayan boslukta yayilan duzlemsel yercekim dalgalarindaki (pp-dalgalar) kaotik davranislarini, asimtotik-analitik ve sayisal metodlar ile gosterdik. Pp-dalgalarinin metrigini kullanarak urettigimiz kaotik Hamilton sistemi, gercek duzlemsel koordinatta ve faz uzayindaki $n \geq 3$ oldugunda karsilik gelen akislari unlu Hénon-Heiles ailesine ait oldugunu gosterdik. Hamilton akisinin integre edilebilme kosullarini incelememiz bize pp-dalgalari gibi basit ve cok iyi bilinen bir dinamigin bile kompleks bir durumda gelisebilecegini gostermektedir.

Approval of the Institute of Research and Graduate Studies

_____

Assoc.Prof.Dr. Zeka MAZHAR

Director of the Intitute

I certify that this thesis satisfies all the requirements as a thesis for the degree of Master of Arts and Sciences.

_____

Assoc.Prof.Dr.Eser AYDIROGLU

Chairman of the Department

We certify that we read this thesis and that in our opinion it is fully adequate, in scope and quality, as a thesis for the degree of Master of Science in Physics.

_____

Prof.Dr.Mustafa HALILSOY

Supervisor

Examining Committee in Charge:

Prof.Dr Mustafa HALISOY. _____

Assoc.Prof.Dr Eser AYDIROGLU _____

Asst.Prof.Dr.Ozay GURTUG _____

Contents

1.Introduction.....1

1.1 Hamiltonian Systems.....3

1.1 Phase-Space and it's Hamiltonian.....3

1.2 Integrable Systems.....5

1.2.1 Constants of Motion and Poisson Brackets.....5

1.2.2 Invariant Tori and Action-Angle Variables.....6

1.3 Origin of Chaos : Hamiltonian Systems.....7

1.3.1 Surface of Section of Hénon-Heiles Type Hamiltonian.....8

2. Geodesics in pp-waves.....10

2.1 Plane-Fronted Gravitational Waves.....10

2.2 The Action Principle for a Relativistic Particle.....12

2.3 Derivation of Geodesic Equations.....13

3.Chaos in pp-waves.....15

3.1 Chaotic Hamiltonian Dynamics from Geodesic Equation.....15

3.2 Hènon-Heiles Hamiltonian.....19

3.3 Numerical Demostration of Chaos in Non-homogeneous pp-waves.....20

3.3.1 Potential function in case of n=2: Homogeneous pp-waves.....20

3.3.2 Polynomial n-saddle Potential Function in case of n=3.....23

3.3.3 Polynomial n-saddle Potential Function in case of n=4.....28

3.3.4 Polynomial n-saddle Potential Function in case of n=5.....32

3.3.5 Polynomial n-saddle Potential Function in case of n=6.....37

3.3.6 Polynomial n-saddle Potential Function in case of n=7.....41

3.4 Asymtotic Analytic Solution in Polar Coordinates....46

3.4.1 Local Solution: In Case of n=3....48

3.4.2 Global Solution....50

4.Conclusion....52

Apendices:

1 MapleV Source Codes....55

1.1 Hènon-Heiles Poincare Mapping....55

1.2 Hamilton Equations : N-Saddle Hamiltonians....56

1.3. Visualization of Geodesic Equations....56

References....58

List of Figures

1.1 .....Poincarè sections of Hénon and Heiles system plane { p_2, q_2 } at $q_1 = 0$ with constant energies.(E = 1/24,1/18,1/12,1/8,1/7,1/6)....9

3.1.....The shape of the potential in real-coordinates when parameter n=3.....17

3.2.....The shape of the potential in real-coordinates when parameter n=4.....18

3.3.....The shape of the potential in real-coordinates when parameter n=5.....18

3.4.....Geodesic motion, for n=1 from rest.....21

3.5.....Geodesic motion, for n=1 from $\dot{x}\ (0) = 2$ and $\dot{y}\ (0) = 1$. 21

3.6.....Geodesic motion, for n=2 from rest.....22

3.7.....Geodesic motion, for n=2 from $\dot{x}\ (0) = 2$ and $\dot{y}\ (0) = 0$ 22

3.8.....Geodesic motion, for n=3 from rest.....24

3.9.....Geodesic motion, for n=3 from $\dot{x}\ (0) = 2$ and $\dot{y}\ (0) = 1$.....24

3.10...Geodesic motion, for n=3 from $\dot{x}\ (0) = 3.1$ and $\dot{y}\ (0) = 0.1$.....25

3.11...Geodesic motion, for n=3 from $\dot{x}\ (0) = 3$ and $\dot{y}\ (0) = 0$.....25

3.12...Geodesic motion, for n=3 from $\dot{x}\ (0) = 0$ and $\dot{y}\ (0) = 3$.....26

3.13...Phase-Space $\{P_x, x\}$, n=3 from rest.....26

3.14...Phase-Space $\{P_y, y\}$, n=3 from rest.....27

3.15...Phase-Space $\{P_y, y, x\}$,n=3 from rest.....27

3.16...Geodesic motion, for n=4 from rest.....29

3.17...Geodesic motion, for n=4 from $\dot{x}\ (0) = 0$ and $\dot{y}\ (0) = 2$.....29

3.18...Geodesic motion, for n=4 from $\dot{x}\ (0) = 2$ and $\dot{y}\ (0) = 0$.....30

3.19...Geodesic motion, for n=4 from $\dot{x}\ (0) = 5$ and $\dot{y}\ (0) = 4$.....30

3.20...Phase-Space $\{P_x, x\}$, n=4 from rest.....31

3.21...Phase-Space $\{P_y, y\}$, n=4 from rest.....31

3.22...Phase-Space $\{P_y, y, x\}$,n=4 from rest.....32

3.23...Geodesic motion, for n=5 from rest.....33

3.24...Geodesic motion, for n=5 from $\dot{x}\ (0) = 0.9$ and $\dot{y}\ (0) = 2.1$.....34

3.25...Geodesic motion, for n=5 from $\dot{x}\ (0) = 2.8$ and $\dot{y}\ (0) = 1.5$.....34

3.26...Geodesic motion, for n=5 from $\dot{x}\ (0) = 3.5$ and $\dot{y}\ (0) = 1.1$.....35

3.27...Phase-Space $\{\mathrm{P}_x, x\}$, n=5 from rest.....35

3.28...Phase-Space $\{\mathrm{P}_y, y\}$, n=5 from rest.....36

3.29...Phase-Space $\{\mathrm{P}_y, y, x\}$,n=5 from rest.....36

3.30...Geodesic motion, for n=6 from rest.....38

3.31...Geodesic motion, for n=6 from $\dot{x}\ (0) = 2$ and $\dot{y}\ (0) = 0.1$.....38

3.32...Geodesic motion, for n=6 from $\dot{x}\ (0) = 3.5$ and $\dot{y}\ (0) = 0$.....39

3.33...Geodesic motion, for n=6 from $\dot{x}\ (0) = 4$ and $\dot{y}\ (0) = 1.2$.....39

3.34...Phase-Space $\{\mathrm{P}_x, x\}$, n=6 from rest.....40

3.35...Phase-Space $\{\mathrm{P}_y, y\}$, n=6 from rest.....40

3.36...Phase-Space $\{\mathrm{P}_y, y, x\}$,n=6 from rest.....41

3.37...Geodesic motion, for n=7 from rest.....42

3.38...Geodesic motion, for n=7 from $\dot{x}\ (0) = 0$ and $\dot{y}\ (0) = 2$.....43

3.39...Geodesic motion, for n=7 from $\dot{x}\ (0) = 1.1$ and $\dot{y}\ (0) = 0$.....43

3.40...Phase-Space $\{\mathrm{P}_x, x\}$, n=7 from rest.....44

3.41...Phase-Space $\{\mathrm{P}_y, y\}$, n=7 from rest.....44

3.42...Phase-Space $\{\mathrm{P}_y, y, x\}$,n=7 from rest.....45